ABSTRACT

Title of Document: SEDIMENT BIOGEOCHEMISTRY ACROSS THE PATUXENT RIVER ESTUARINE GRADIENT: GEOCHRONOLOGY AND FE-S-P INTERACTIONS

Jennifer A. O'Keefe, M.S., 2007

Directed By: Associate Research Professor Jeffrey Cornwell, Marine Estuarine Environmental Sciences

Although salinity and redox gradients are defining features of estuarine biogeochemistry, compositional changes in sediment characteristics associated with these factors are poorly described in U.S. coastal plain estuaries. Understanding the basics of nutrient sources and sinks, in the context of these defining characteristics, is required to make efficient and effective management decisions regarding estuarine eutrophication. In this study, detailed analysis of long-term nutrient burial has been used as a tool to understand the trajectory of nutrient cycling at 7 stations along an oligohaline to mesohaline transect in the Patuxent River estuary. Sediment mass accumulation rates were determined for 3 of the 7 sites. Cores analyzed for total P, total N, organic C, biogenic silica, $\delta^{13}C$, and $\delta^{15}N$ did not provide evidence of historical nutrient reduction actions taken in this watershed. Burial rates of Fe-S mineral phases and inorganic P (IP) indicated pyrite formation limited the availability of Fe-oxides for adsorption and retention of IP.

SEDIMENT BIOGEOCHEMISTRY ACROSS THE PATUXENT RIVER ESTUARINE GRADIENT: GEOCHRONOLOGY AND FE-S-P INTERACTIONS

By

Jennifer A. O'Keefe

Thesis submitted to the Faculty of the Graduate School of the
University of Maryland, College Park, in partial fulfillment
of the requirements for the degree of
Master of Science
2007

Advisory Committee:
Associate Research Professor Jeffrey Cornwell, Chair
Professor Walter Boynton
Associate Professor Judith Stribling

Acknowledgements

Funding for this research was provided by the National Science Foundation (grant DEB-0235884 awarded to Dr. Thomas Jordan, Dr. Walter Boynton, and Dr. Jeffrey Cornwell). Additional support was provided by Horn Point Laboratory, University of Maryland Center for Environmental Science. Thanks to Dr. Jeffrey Cornwell, my Master's research advisor, and members of my Master's research committee, Dr. Walter Boynton and Dr. Judith Stribling, for guiding the focus of this research and for helpful insights along the way. Thanks to Michael Owens, Erica Kiss, Rebecca Holyoke, Jeremy Testa, Lois Lane, Sara Rhoades, Sarah Greene, and Dr. John Anderson for field and laboratory assistance. Additionally I would like to thank my family, friends, and especially Steve for providing support and encouragement throughout my graduate experience.

Table of Contents

List of Tables

List of Figures

CHAPTER 1: SEDIMENT GEOCHRONOLOGY OF SUB-TIDAL NUTRIENT BURIAL IN THE SALINITY TRANSITION ZONE OF THE PATUXENT RIVER, USA

ABSTRACT

Development of a basic understanding of nutrient sources and sinks is required to make efficient and effective management decisions regarding estuarine eutrophication. In this study, detailed analysis of long-term nutrient burial has been used as a tool to understand the trajectory of nutrient cycling at 7 stations along an oligohaline to mesohaline transect in the Patuxent River estuary. Sediment mass accumulation rates (MAR) for collected cores (30 cm ≤ length ≤ 103 cm) were difficult to determine for tidal fresh and oligohaline sites; however, MAR from site 3 (oligohaline) indicated sedimentation could range from 6656 to 18,105 g m^{-2} y^{-1} in this portion of the estuary. Mesohaline sediment MARs (1761-2291 g m^{-2} y^{-1}) were similar to previous studies in the lower estuary. Cores analyzed for total P, total N, organic C, biogenic silica, $\delta^{13}C$, and $\delta^{15}N$ did not provide evidence of historical nutrient reduction actions taken in this watershed.

INTRODUCTION

Eutrophication in estuarine and coastal waters is predominantly a result of anthropogenic changes in nutrient cycling (Nixon 1995; Cloern 2001, Fisher et al. 2006). Effects of eutrophication include increased incidence of algal blooms, loss of submerged aquatic vegetation, and low oxygen concentrations (Cloern 2001; Stankelis et al. 2003; Breitburg et al. 2003; Kemp et al. 2005). Although eutrophication of coastal and estuarine environments has been identified in the Chesapeake Bay and its tributaries for a considerable amount of time, studies of nutrient cycling have substantial room for improvement and elaboration.

Although box-models are useful tools for summarizing nutrient transportation, regeneration, and cycling process in coastal and estuarine environments (e.g. Testa 2006), estuarine nutrient sequestration is often one of the most poorly constrained variables in box-modeling and mass balance approaches (Boynton et al. 1995; Boynton et al. *in prep.*). Despite differences in sediment sources, transport/resuspension dynamics, and chemistry within estuarine gradients (i.e. from fluvial sources to mesohaline waters), it is not uncommon to characterize large areas of estuarine sediment with dated cores collected from relatively few sampling locations (e.g. Khan and Brush 1994; Cornwell et al. 1996, Zimmerman and Canuel 2002). Additionally, due to the difficulties associated with temporal variation of fluvial inputs, resuspension and physical/biological mixing, estimates of mass accumulation rates in upper estuarine sub-tidal sediments are limited. Few studies have attempted to characterize variability in sediment mass accumulation or sediment nutrient burial within the context of this gradient.

The Patuxent River, a sub-estuary of Chesapeake Bay, was chosen for this study because of the history of biogeochemical studies (D'Elia et al. 2003) and considerable management actions taken in this system in an attempt to remedy excessive nutrient inputs (i.e. Fisher et al. 2006; Boynton et al. *in prep*.). Relatively comprehensive box-models of sediment and nutrient mass balance estimates have been published for the Patuxent River (Boynton et al. 1995; Hagy et al. 2000); these studies have emphasized nutrient cycling in the water column, marsh sediments, and sub-tidal surface sediment (Fisher et al. 2006; Merrill 1999; Boynton et al. 1995; Jordan et al. *in press*). Long-term nutrient burial rates within the estuary are largely unmeasured, though rates are available for marshes (Greene 2005; Merrill 1999; Kahn and Brush 1994) and limited sub-tidal mesohaline environments (Adelson 1997, Kahn and Brush 1994, Cornwell *unpubl. data*). This study extends the characterization of sediment and nutrient burial to the salinity transition zone of the Patuxent River estuary encompassing tidal fresh, oligohaline, and mesohaline environments. The salinity transition zone, located between 30 and 60 km above the mouth of the Patuxent River, is a region of distinct variability in the defining physical and chemical characteristics of estuarine systems (Jordan et al. *in pres*s). The dynamics of long-term nutrient burial in the context of the physical and geochemical characteristics of the estuary can be used to refine nutrient budgets and strategies for remediation.

This study examined geochronology within the salinity transition zone of the Patuxent River sub-estuary. I addressed 4 questions relevant to processes highlighted by the estuarine salinity gradient:

1. Are sediment mass accumulation rates and nutrient burial rates homogenous?

2. Have sediment mass accumulation rates and nutrient burial rates changed over time?
3. Are anthropogenic influences on sediment mass accumulation rates and nutrient burial rates evident in dated sediment?
4. What are the ecological implications of spatial and temporal variability in nutrient burial rates?

METHODS

Study Site Description

The 2,393 km^2 watershed of the Patuxent River is located entirely in the state of Maryland, USA; dominant land uses are forests and medium density residential development (MDP 2000). The study area focused on the salinity gradient of the Patuxent River sub-estuary, encompassing the salinity transition zone (Fig. 1.1). Seven sub-tidal locations were chosen for coring with salinities ranging from freshwater to mesohaline. Water column depths in the study area averaged less than 10 m. Although deeper waters of the lower estuary may experience stratification and hypoxia, fresh and oligohaline waters are vertically well mixed and aerobic (Lung and Bai 2003; Hagy et al. 2000) as are the shallow sub-tidal areas chosen for mesohaline core collection in this study. In general, sediment grain size is dominated by silt and clay (Cornwell *unpubl*. data). Average ash-free dry weight (determined as the difference between dried sediment and sediment that has been combusted at 550° C for 120 min.) for the top 5 cm of collected sediment cores ranged from 4% to 15 % (Table 1.1). Average water content of collected sediment cores ranged between 29% and 85% (Table 1.1).

Sample Collection and Preparation

Sediment cores (30 cm < core length < 105 cm) were collected in June and August 2004 from 7 shallow sub-tidal locations (water column depth < 7 m) within the salinity transition zone of the Patuxent River sub-estuary (Table 1.1). Sediment cores were collected using a hand-deployed piston corer (8 cm inner diameter; Abysmal Corers, Colorado). Cores were transported to the laboratory where they were sectioned within 48 hours of collection. The sediment was sectioned into intervals of 1.0 cm (0-10 cm depths), 2.0 cm (10-30 cm depths), 5.0 cm (30-60 cm depths), or 10.0 cm (60-100 cm depths). Sediment sections were homogenized in polypropylene beakers; sub-samples from each section (approximately 10mL wet volume) were stored in low density polyethylene snap-cap vials and frozen for analysis of reduced iron sulfide minerals (Chapter 2). The remaining sediment was placed in aluminum pans and dried in a forced-air oven at 80°C. Sediment samples were dried to a constant weight, ground by hand (using a porcelain mortar and pestle), and stored in plastic bags at room temperature for further analysis.

Geochemical Analysis

Sedimentation Mass Accumulation

The sediment mass accumulation rate (MAR) for each core was determined using ^{210}Pb radionuclide analyses. The analysis of ^{210}Pb ($T_{½}$ = 22.3 yr) was carried out via the analysis of its daughter radionuclide ^{210}Po ($T_{½}$ = 138 days). Sediment sections were digested and analyzed for ^{210}Pb following Cornwell et al. (1996); secular equilibrium between ^{210}Pb and ^{210}Po was assumed. Profiles of ^{210}Pb (or ^{210}Po) activity in aquatic sediments consist of two main components: 1) "excess" or "unsupported" ^{210}Pb and 2)

"supported" or background ^{210}Pb. Excess ^{210}Pb is that component of ^{210}Pb that is in excess of the ^{210}Pb generated *in situ* via the decay of ^{226}Ra (i.e. supported; Robbins 1978). In this study ^{226}Ra concentrations are estimated from the asymptotic ^{210}Po concentrations at depth.

The decay of radionuclides is a first order process described by the equation:

1) $A = A_0 e^{-kt}$

Where A is the activity at time t, A_0 is the activity at time zero and k is the decay coefficient (0.03114 for ^{210}Pb). This equation may be modified for sediments:

2) $A = A_0 e^{(-kx/w)}$

Where A is the activity (dpm g^{-1}) at depth x (cm) and w is the sediment accumulation rate (cm yr^{-1}). In most sedimentary situations, the percent water of the sediment may vary down core. The amount of sediment in each section (g cm^{-3}) can vary considerably, generally increasing with sediment depth because of compaction. An alternative scale can be used to correct for this effect, using cumulative mass (g cm^{-2}) rather than depth (cm). In this study, we use cumulative mass rather than depth which yields a sediment accumulation rate in units of g cm^{-2} y^{-1}.

For ^{210}Pb based sedimentation, this formulation is termed the **c**onstant **i**nitial **c**oncentration model (CIC). Calculation of sediment accumulation rates based on this model requires several assumptions: 1) constant input fluxes of sediment and excess ^{210}Pb, 2) no post depositional mobility of ^{210}Pb relative to sediment particles, and 3) no sediment mixing by biota or physical processes. In the ideal situation, excess ^{210}Pb is described by equation 2 and provides an exponential decrease in excess ^{210}Pb activity with depth. To apply this model, equation 2 is log transformed:

3) $\ln A = \ln A_0 - (kx/w)$

The term k/w is determined from the slope of the linear regression of x and ln A ($\ln A_0$ is the intercept). In this study, sediment mass accumulation rates were not determined for core regressions with $p > 0.05$. In several cases, cores were apparently too short to determine the total ^{210}Pb inventory and thus excess ^{210}Pb activity could not be determined.

To estimate the age at specific sediment depths, the cumulative mass at the specified depth was divided by the sedimentation rate. Because the CIC model requires constant ^{210}Pb inputs and constant sedimentation rates, the output from this model yields a constant sedimentation rate for the entire length of a sediment core profile. The Constant Rate of Supply (CRS) model (Appleby and Oldfield 1978) accommodates variable rates of sedimentation at different depths (data not shown), but provided little advantage over the CIC model.

Based on known regional atmospheric inputs of ^{210}Pb (Kim et al. 2000), sediment cores with total ^{210}Pb inventories greater than 25 dpm cm^{-2} were considered to be collected from sites experiencing focused sedimentation. Similarly cores with total ^{210}Pb inventories less than 25 dpm cm^{-2} were considered to be collected from sites inefficient at trapping particles. Sediment accumulation rates were corrected for these differences in particle trapping by dividing the ^{210}Pb inventory for the core by the expected inventory (25 dpm cm^{-2}) and multiplying this factor by the accumulation rate determined from the CIC model.

Nutrient and Stable Isotope Analysis

Total phosphorus was extracted from ashed sediment using 1N HCl (Aspila et al. 1976) and analyzed colorimetrically (Parsons et al. 1984). Biogenic silica (BSi), was determined by dissolving silica in the sediment matrix in a weak Na_2CO_3 base over a 3 hour time course (DeMaster 1981); dissolved silica was analyzed colorimetrically (Lane et al. 2000). Sediment samples analyzed for carbon and nitrogen isotopes were acidified with 1 N HCl and shaken for 15 minutes to remove any carbonates. Samples were centrifuged and the HCl was decanted; samples were washed with deionized water, centrifuged, and decanted three times to remove acid. Dried sediment samples were analyzed for nitrogen and carbon isotopic composition (University of California, Davis, Stable Isotope Facility).

RESULTS

Sediment Mass Accumulation Rate

Cores from 3 of the 7 sampling locations were successfully dated. Profiles of ^{210}Pb activity from two oligohaline sites (site 3 and site 6) as well as the mesohaline site (site 7) are shown in Fig. 1.2. A linear regression of the natural log of excess ^{210}Pb activity and the cumulative mass of specific sediment sections described a significant relationship ($p \leq 0.01$) for cores collected from these sites (Fig. 1.3). The slope of this regression was used to determine sediment mass accumulation rates for these three cores (Table 1.2). Mass accumulation rates at sites 6 and 7 were similar (~350 g m^{-2} y^{-1} difference) while the mass accumulation rate calculated for site 3 was more than 8 times greater than the other sites dated.

The ^{210}Pb inventories from sites 6 and 7 were generally as expected from ^{210}Pb atmospheric input (~25 dpm cm^{-2}; Kim et al. 2000). Although the inventory from site 6

(26 dpm cm^{-2}) suggested a modest amount of sediment focusing while a slight particle trapping inefficiency was indicated by the inventory from site 7 (24 dpm cm^{-2}; Table 1.2). The ^{210}Pb inventory from site 3 (68 dpm cm^{-2}) suggested substantial sediment focusing. After correcting for sediment focusing, the mass accumulation rate at site 3 was reduced (Table 1.2); however, it was still 3 times greater than mass accumulation rates at other dated sites.

Sedimentation rates from 4 of the 7 collected cores were not able to be determined. Two of these "un-dateable" sites were located in the middle of the study area (site 4 and site 5), one site was located at the tidal freshwater end of the transect (site 1) and one site was located at the tidal fresh-oligohaline boundary (site 2). Profiles of ^{210}Pb activity from sites 1, 2, 4, and 5 suggested that these locations are influenced by mixing processes as well as by high sedimentation rates (data not shown). A clear asymptote, indicating the background $^{226}Ra/^{210}Pb$ activity, was not discernable in ^{210}Pb activity profiles from these sites. Due to the additional influences on sediment accumulation apparent at these sites, longer sediment cores would be required to determine the background ^{210}Pb activity.

Sediment Nutrient Accumulation and Ecological Indicators: Trends in Geochronology

Due to the more moderate mass accumulation rate determined for the core collected from site 7 (and thus longer chronological span), this core was chosen for further analysis of geochronological trends in nutrient burial. Profiles of nutrient accumulation are useful in describing chronological changes in nutrient sequestration. Sediment core profiles,

particularly sediment horizons < 50 years old, may be compared to known changes in anthropogenic nutrient inputs.

In 1985 phosphate detergents were banned in the state of Maryland, and sewage treatment plants in the Patuxent River watershed began removing P in 1986. Although profiles of total phosphorus (TP) concentrations showed a slight decline between 1980 and 1990 (Fig. 1.4A), overall TP concentrations increased ~2.5-fold over the length of the core. Despite recent improvements, wastewater treatment technology is not keeping up with increasing P inputs that result from increased population in the watershed.

The history of N loading is a balance between increased loading from non-point sources and decreased inputs from point sources (Fisher et al. 2006). Fisher et al. (2006) have described an increase in the use of inorganic nitrogen fertilizers in the watershed of the Patuxent River after World War II. Indeed, the total nitrogen (TN) concentrations at site 7 were nearly constant prior to 1940; however between 1940 and 1965 TN concentrations decreased ~1.3 fold (Fig. 1.4A). After 1965, TN concentrations increased steadily until the present (Fig 1.4A). Biological nitrogen removal was implemented in wastewater treatment plants in 1993 (Boynton et al. *in prep*); however, this change in N-loading is not discernable in total nitrogen sediment profiles in this study (Fig. 1.4A).

Similarly, the lowest average organic carbon (org-C) concentrations (19.0 mg g^{-1} ± 1.0 standard deviation) in the sediment profile from site 7 were between 1942 and 1985 (Fig. 1.4B). Average org-C concentrations were similar prior to (22.7 mg g^{-1} ± 1.9) and after (23.4 mg g^{-1} ± 1.7) the 1945-1985 time-period. Overall, most points (70%) in the site 7 sediment history record fall with in the range of concentrations averaged for the entire core (21.5 mg g^{-1} ± 2.4 standard deviation). Three out of four points less than the

average org-C concentration occurred in the 1946-1985 time period, while four out of five points greater than the average were in the deepest and shallowest sediment sections (Fig. 1.4B).

Despite apparent temporal variation in the concentration of nitrogen and carbon accumulation at site 7, the C: N ratio showed little temporal change (Fig. 1.4B). A lack of temporal variation in the profile of the C: N ratio indicates that observed variation in the profiles of org-C and TN may be attributed to compositional changes in these buried nutrients rather than to variation in sedimentation rates. For example, if the observed peak in org-C concentration at 1914 (24.5 mg g^{-1}) were attributable to greater sedimentation during that time-period, one would expect to see a concurrent peak in the TN profile. However, the buried TN concentration at this time point (2.2 mg g^{-1}) was equal to points buried prior to and after 1914. Although the overall C: N ratio profile is driven by changes in sedimentary carbon accumulation, differences in compositional changes may only be observable in profiles of the individual nutrient pools. Further evidence of changes in nutrient burial may be gleaned from sedimentary profiles of biogenic silica and stable isotopes which may provide an indication of differences in ecological functioning throughout the chronological span of the core.

Anthropogenic nutrient enrichment can be difficult to discern in some estuarine sediment nutrient profiles (Cornwell et al. 1996); this is especially true in the case of phosphorus, which is often adsorbed onto particles that are transported throughout the estuary. However, changes in sediment accumulation of certain biomarkers may provide indicators of changes induced in ecological processes as a result of eutrophication (Zimmerman and Canuel 2002). For example, biogenic silica (BSi) is less mobile than

some other nutrients (such as P); it is often deposited in sediments in close proximity to where it is taken up for incorporation into diatom frustules (Conley et al. 1993). Therefore, observations of changes in biogenic silica (BSi) in sediment profiles may provide more accurate measurement of eutrophication than nutrient profiles alone.

Until 1970, the concentration of accumulated BSi was relatively constant at site 7 (Fig. 1.4B; average 5.73 mg g^{-1} ± 0.89 standard deviation). Beginning ~1970 until the mid-1990s, average BSi concentrations (2.3 mg g^{-1} ± 0.51 standard deviation) were ~2.5-fold less than concentrations found in historic sediments. However, concentrations of BSi burial in the past decade were more consistent with historical BSi concentrations.

Although sediment profiles of BSi indicated distinct differences in production throughout the historical span of the site 7 core, sediment isotopic characterization indicated a relatively constant carbon signature over the history of the core. Values of $\delta^{13}C$ ranged between -23.25‰ and -24.63‰. Of the 27 data points analyzed from the site 7 core, 16 data points (59%) were in the range of -24.0‰ and -23.70‰. Points less than -24.0‰ correspond to the 1904 and 1924 time points as well as sub-surface sediment depths (0 to 9cm; 9 data points) corresponding with the 1987 to 2003 time period (Fig. 1.5B). Points greater than -23.70‰ correspond with the 1973 and 1976 time points. The $\delta^{13}C$ signature of sediments may be influenced by several mechanisms including 1) mixing of particulate carbon from different sources (terrestrial, marine, marsh), 2) changes in carbon sources (as from a land-use shift from C3 plants to C4 plants in terrestrial sources) 3) phytoplankton assimilation of HCO_3^- due to CO_2 limitation (as a result of eutrophication and high productivity), and 4) post-depositional diagenesis (Bratton et al. 2003). Despite the few variations described above, the sedimentary $\delta^{13}C$

profile from site 7 was quite constant over the geochronological span of the core. The $\delta^{13}C$ profile indicates terrestrial sources dominated the carbon pool at site 7 (typical $\delta^{13}C$ value of terrestrial organic carbon is -25‰).

Similar to $\delta^{13}C$, site 7 $\delta^{15}N$ profiles indicated terrestrial sources dominate the nitrogen pool. Site 7 $\delta^{15}N$ values ranged between 4.56 and 8.58‰. Unlike the TN profile from site 7, the $\delta^{15}N$ profile exhibited constant and steady enrichment from ~1900 until the present (Fig. 1.5A). Because organic matter decomposition preferentially removes ^{14}N (Bratton et al. 2003), one would expect sub-surface sediment sections, that have yet to undergo complete decomposition, to be more enriched than deeper sediments. However, the profile from site 7 indicated increasing enrichment of the sedimentary N isotopic signature has been occurring since the early 20th century. Thus, isotopic N enrichment can not be explained by a lack of decomposition alone.

DISCUSSION

Comparison of Shallow Sub-tidal Sediment and Nutrient Accumulation Rates in the Patuxent River Estuary to Other Accumulation Studies

This study adds a new component to the understanding of sediment dynamics in this ecosystem. Sediment cores collected from several sites in this study were characterized by modest sediment focusing, with site 3 exhibiting the greatest mass accumulation rate (between 3 and 8 times greater than the mass accumulation rate at site 6). Although this may be an indication that the salinity transition zone is a region of sediment focusing in the Patuxent River estuary, further study of sedimentation rates in this area would be necessary to determine the amount of homogeneity in sediment mass accumulation. Such

studies should be certain to include horizontal transects within specific areas of interest in order to account for physical influences on sediment deposition.

Calculated sediment mass accumulation rates and nutrient burial rates for the sub-tidal mesohaline Patuxent River (Table 1.3) were within the range of rates determined for the mesohaline main stem Chesapeake Bay (Table 1.4). Site 3 from this study was characterized by greater nutrient burial rates; however, this may be attributed to focused sedimentation at the location of core collection

Different sediment accumulation studies in the Patuxent River estuary yielded several differences between marsh and sub-tidal sediment mass accumulation dynamics (Table 1.3).

1. Mass accumulation in tidal freshwater and oligohaline marshes is more variable than mass accumulation in the neighboring sub-tidal areas. This may be the result of spatial differences in marsh accretion driven by either riverine inputs of terrestrial particles or via accumulation of organic matter (i.e. Merrill and Cornwell 2000).
2. Sub-tidal and marsh sediment nutrient burial in the oligohaline estuary appear to be of similar magnitude.
3. Since a large proportion of Patuxent River marshes are located in the oligohaline portion of the estuary (80%; Boynton et al. *in prep*.), one may conclude that these areas may play a more important role in sedimentation and nutrient burial than fresh/oligohaline sub-tidal areas. Likewise, sediment accumulation and nutrient burial in sub-tidal areas may be more important

than in marshes in the mesohaline Patuxent River estuary due to a greater percentage of open-water in this portion of the estuary.

Although sediment cores from the oligohaline portion of the estuary (this study) exhibited greater nutrient burial rates than those from the lower mesohaline portion (Boynton et al. *in prep*), the mesohaline portion of the estuary accounts for a greater proportion of the Patuxent River estuary. Thus, on a total aerial basis, mesohaline sediments may play a more important role in Patuxent River sub-tidal nutrient burial than fresh and oligohaline sub-tidal sediments.

Historical and Spatial Differences in Nutrient Burial and Ecological Indicators

Ecological indicators suggested changes in nutrient loading may have affected primary production in the mesohaline portion of the Patuxent River estuary. The sedimentary profile at site 7 indicated a trend toward declining BSi accumulation since the mid-20th century. This time period coincides with increased TP accumulation, decreased TN accumulation, and an increasing $\delta^{15}N$ signature in the sedimentary profile. Other investigations have documented increasing BSi burial in recent sediments (Cooper 1999; Colman and Bratton 2003). The declining BSi concentrations observed at site 7 may be an indication that primary production has shifted to other locations in the estuary. Since sedimentary BSi may be used as an index of diatom deposition (Conley 1988), increasing BSi burial in sediments indicates greater water column production, which may be attributable to increases in nutrient availability (Smith 2006) due to cultural eutrophication (Fisher et al. 2006).

In eutrophic conditions, the Si cycle may be altered by two mechanisms: 1) increased nutrients will change the Si:N and Si:P ratios and thus may alter ecosystem dynamics; and, 2) increased nutrients may lead to increased diatom production and thus increased deposition and preservation of diatoms in the sediment (decreasing water column Si concentrations; Conley et al. 1993). Increases in nutrient inputs may have reduced primary production limitation in the oligohaline portion of the estuary, thus allowing for phytoplankton blooms to occur in this part of the estuary. In such a situation, nutrient resources may be exhausted in upper estuarine blooms as greater production in the water column would lead to greater Si, N and C deposition to sediments (Rabouille et al. 2001). Thus production further down estuary may be nutrient limited. Indeed general observations of sedimentary nutrient concentrations indicated BSi, TP, TN, and org-c accumulation is greater in oligohaline sediments than in sediments from site 7 (Fig. 1.6). However, further analysis of dated sediment cores would be needed to determine if a historical shift, associated with changes in nutrient inputs from the watershed, has indeed occurred at these locations.

CONCLUSIONS

Sediment dating in the tidal fresh and oligohaline portion of the Patuxent River estuary was difficult due to rapid sediment accumulation, bioturbation by macrofaunal species, and the physical mixing of particles in this shallow water system. Despite these difficulties, some key findings in upper estuarine sediment and nutrient accumulation have been determined:

1) Sediment mass accumulation rates in the tidal fresh and oligohaline portion of the estuary are not homogenous and exhibit considerable variation within a relatively constrained area.

2) Sediment mass accumulation rates in the mesohaline portion of the estuary, below the salinity transition zone, are similar to rates calculated at the mouth of the estuary.

3) Although nutrient burial rates in the salinity transition zone of the Patuxent River estuary have exhibited a change over time, these changes do not necessarily reflect key time points in watershed nutrient management in a simple way.

4) Comparisons of sedimentary isotopic characterization and biogenic silica concentrations may be better indicators of changes in ecological functioning than nutrient accumulation profiles alone.

TABLES

Table 1.1 Description of sub-tidal sediment cores collected in the salinity transition zone of the Patuxent River estuary and relevant collection site physical characteristics.

Site Number	Date Collected	Coordinates	Salinity*	Core Length (cm)	Water Column Depth** (m)	Water Content (%)	Ash Free Dry Weight†
1	8/23/2004	38°46.130'N 76°41.967'W	0-0	63	1.0	29 - 55	3.75 ± 4.06
2	6/21/2004	38°41.120'N 76°41.537'W	0-1	93	1.6	58 - 81	15.3 ± 1.71
3	6/21/2004	38°37.677'N 76°40.689'W	0-3	103	1.4	62 - 85	12.2 ± 0.25
4	8/23/2004	38°35.434'N 76°40.316'W	0-4	68	1.5	45 - 64	5.16 ± 0.55
5	8/23/2004	38°33.520'N 76°40.283'W	1-5	30	1.5	70 - 82	12.3± 0.83
6	8/23/2004	38°31.043'N 76°39.778'W	1-8	56	6.0	64 - 49	10.8± 0.73
7	6/21/2004	38°29.313'N 76°40.052'W	3-11	77	2.4	61 - 75	9.25 ± 0.33

[*]Range of the average March through August salinity as monitored by the Chesapeake Bay Program (1990-1998; as reported in Jordan et al. 2007). [**]Water column depth at time of core collection; average water column depths may vary according to tides. [†]Ash-free dry weight was averaged for the top 5 cm of each sediment core.

Table 1.2 Summary of sediment mass accumulation rates determined from ^{210}Pb analysis (calculated from the CIC model) for dated sediment cores from this study.

Site Number	Sedimentation Rate*	^{210}Pb Inventory**	Focus Corrected Sedimentation Rate*
3	18,105	68	6656
6	1831	26	1761
7	2183	24	2291

*Units are g m^{-2} y^{-1}

**Units are dpm cm^{-2}

Table 1.3 Sedimentation rates and nutrient burial rates for Patuxent River estuary sub-tidal areas and marshes. Ranges in rates for marsh studies include transects from high to low marsh. Ranges in rates for sub-tidal areas include estimates corrected for sediment focusing as well as "typical" burial rates. Standard deviations are given for averages from this study.

Source	Accumulation or Accretion Rate*	Total N Burial Rate*	Organic C Burial Rate*	Total P Burial Rate*
		Freshwater to Oligohaline†		
Marsh				
Khan and Brush 1994	300-5600	8-25	30-250	4-2.25
Merrill 1999 (site 5)	8600	25.0	-----	3.82
Merrill 1999 (site 6)	4200	35.4	-----	3.24
Merrill 1999 (site 7)	800	36.1	-----	4.33
Merrill 1999 (site 8)	6900	32.2	-----	10.0
Sub-tidal				
Khan and Brush 1994	200-5900	50-100	30-130	4-12.5
		Oligohaline†		
Marsh				
Merrill 1999 (site 9)	1700	7.56	-----	0.18
Merrill 1999 (site 12)	3300	15.7	-----	1.96
Greene 2005	1160-7900	12.0-32.5	-----	1.3-5.9
Sub-tidal				
This study (site 3)††	6656-18105	62 ± 16	712 ± 158	34 ± 3.4
		Oligohaline to Mesohaline†		
Sub-tidal				
Adelson 1997	2097-8600	-----	-----	-----
This study (site 6)††	1761-1831	-----	-----	1.58 ± 0.53
		Mesohaline†		
Sub-tidal				
Boynton et al. *in press*	1143	-----	-----	-----
This study (site 7)††	2183-2291	4.5 ± 0.52	47 ± 5.1	1.2 ± 0.33

[†]Study areas between 70-60 km from the mouth of the estuary were categorized as "freshwater to oligohaline"; 60-50 km as "oligohaline"; 40-45 km as "oligohaline to mesohaline", and 45-0 km as "mesohaline".

[††]Nutrient burial rates from this study have been averaged based on the uncorrected sedimentation rate for sediment depths 0-55 cm; standard deviations are given.

[*]Units are g m^{-2} y^{-1}

Table 1.4 Sediment mass accumulation rates and nutrient burial rates from mesohaline main stem Chesapeake Bay (total nitrogen, organic carbon, and total phosphorus). Ranges in rates are presented for studies including multiple cores.

Source	Sediment Mass Accumulation Rate*	Total Nitrogen Burial Rate*	Organic Carbon Burial Rate*	Total Phosphorus Burial Rate*	Biogenic Silica Burial Rate*
Cooper and Brush 1991 (8 cores)	0.03-0.31†	0.3-2.8†	2.5-29†	-----	-----
Cornwell et al 1996 (2 cores)	1800-2400	3.6-12	27-84	0.72-2.16	63-168
Zimmerman and Canuel 2000 (1 core)	4770	9-25	71-174	-----	14-143
Zimmerman and Canuel 2002 (2 cores)	1400-12100	-----	30-90	-----	-----

*Units are g m^{-2} y^{-1}

†Units are cm y^{-1}. Authors reported these rates as averages per core; I have given the range of these averages from all cores within that study.

FIGURES

Figure 1.1 Map from Jordan et al. (I*n Press*). Left: The Patuxent River Estuary and its watershed. Right: Enlargement of the upper estuary (30-70 km from the mouth) showing the seven sampling sites.

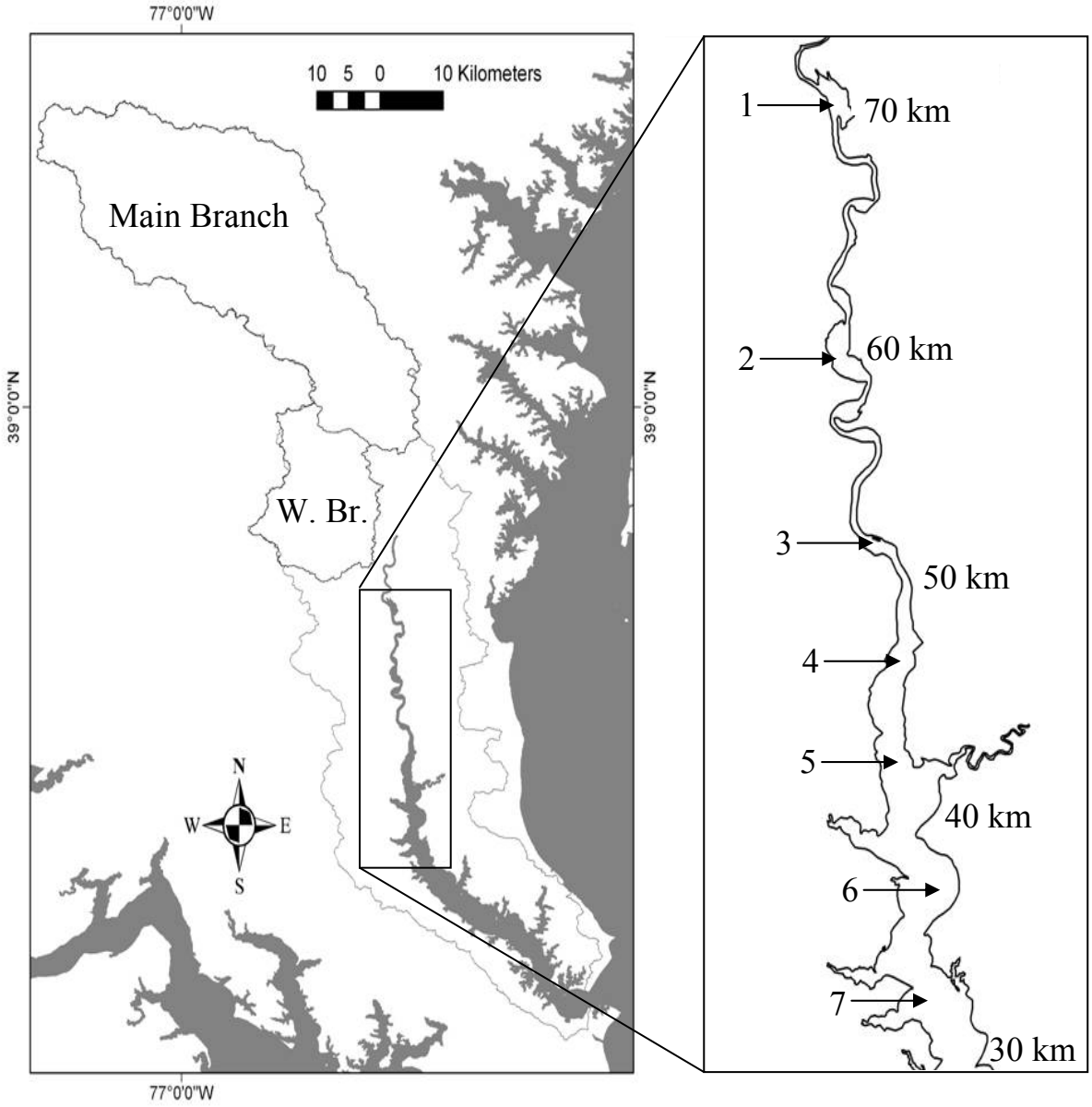

Figure 1.2 Sediment core profiles of ^{210}Pb activity (dpm) at selected depths from Site 3 —■—; Site 6 —▲—; and Site 7 ···⊙···.

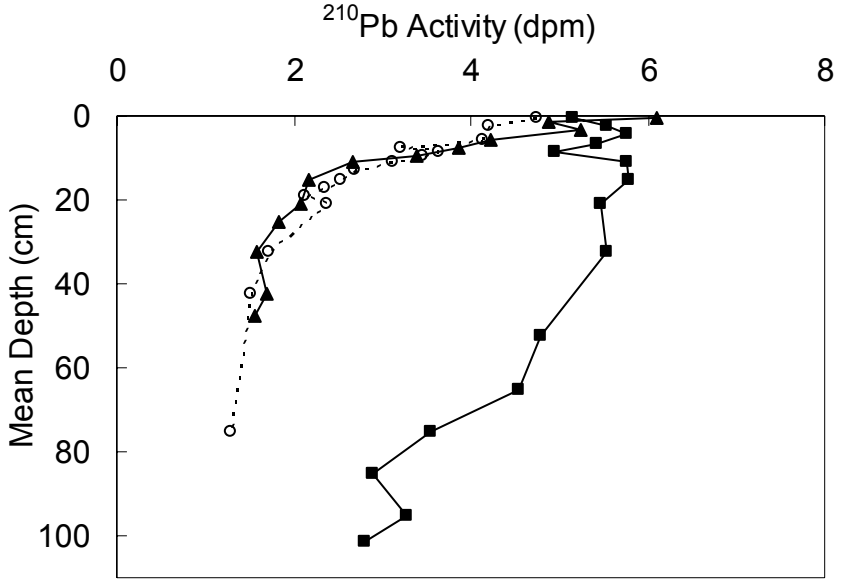

Figure 1.3 Regression of the natural log of excess ^{210}Pb and the cumulative mass for site 3 (A), site 6 (B), and site 7 (C); $p \leq 0.01$ for all regressions.

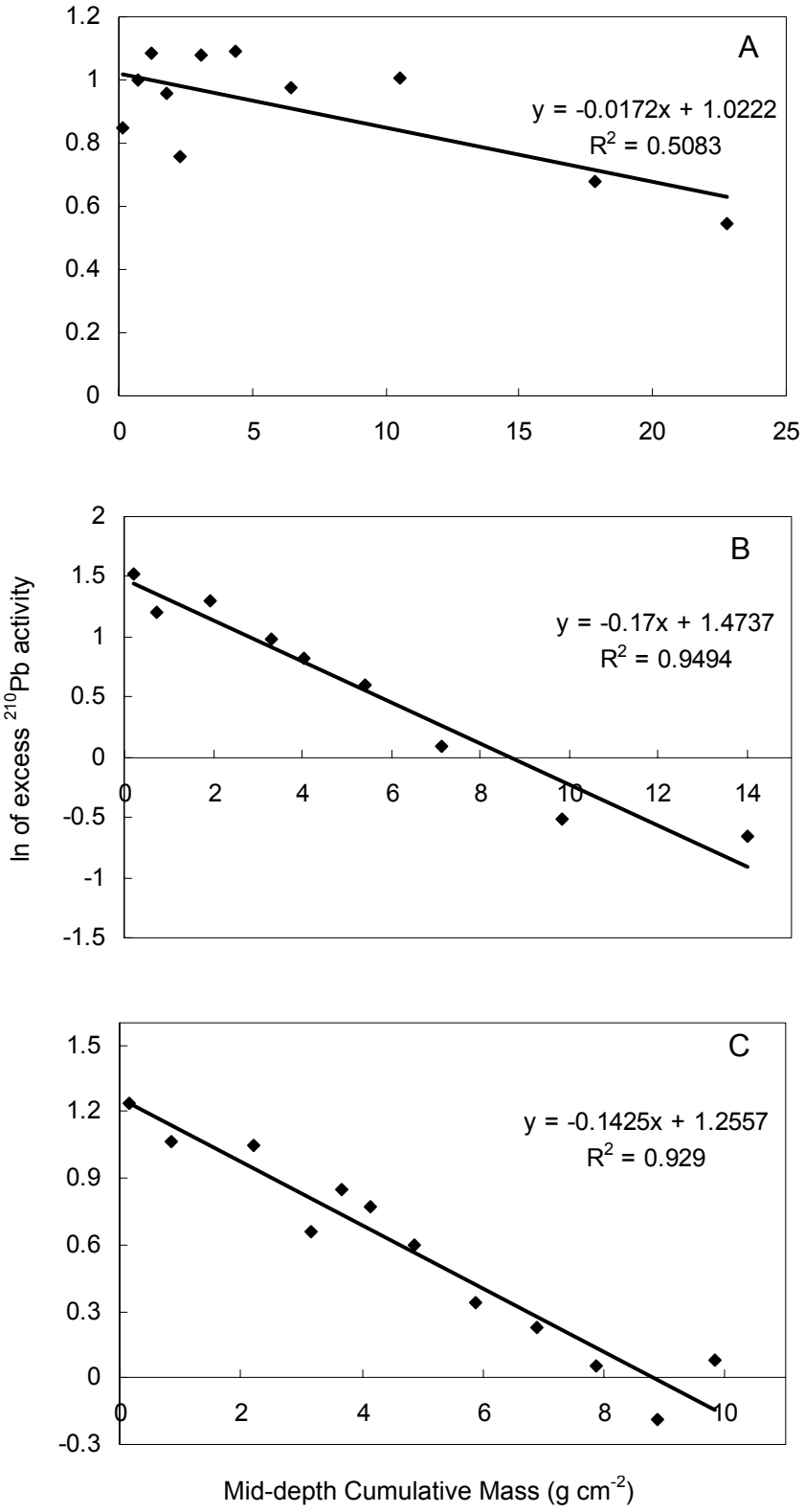

Figure 1.4 Concentration (mg g^{-1}) of (A) total phosphorus —●—, total nitrogen —▲—, (B) biogenic silica —■—, organic carbon —✳—, and C: N ratio —○— at site 7 for calculated dates of sedimentation.

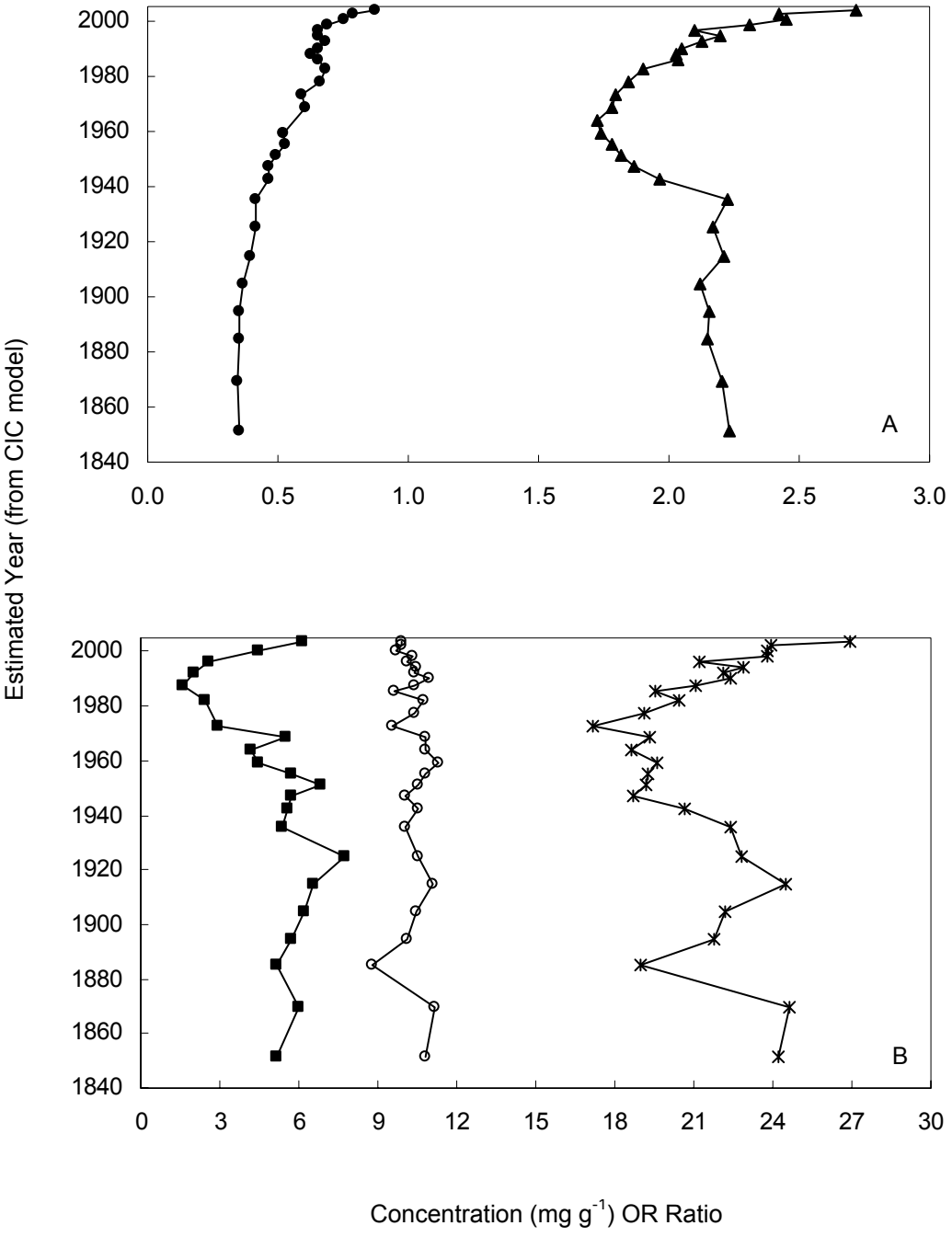

Figure 1.5 Profiles from site 7 of (A) nitrogen and (B) carbon sediment isotopic signature at calculated dates of sedimentation.

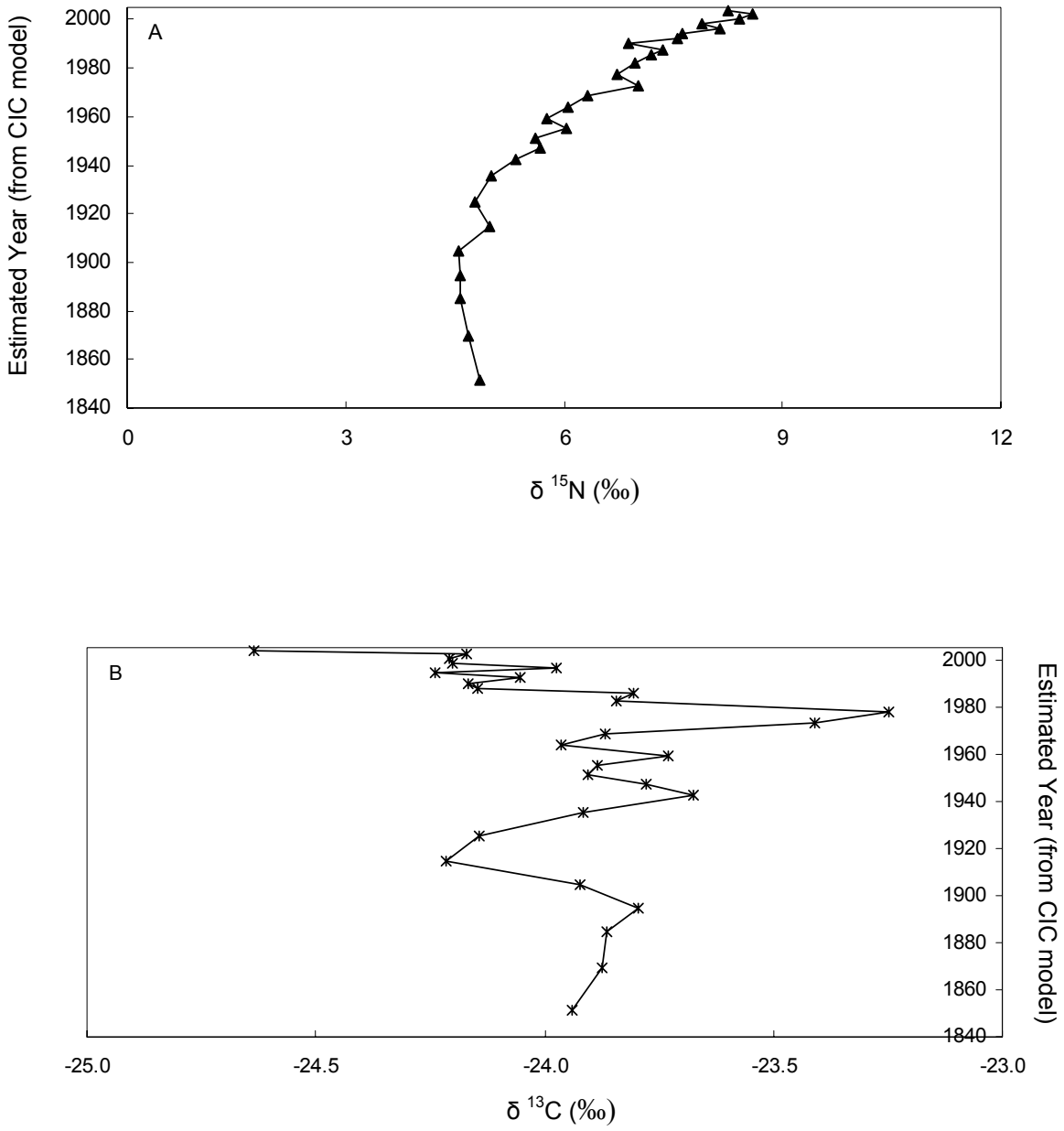

Figure 1.6 Average nutrient concentrations between 0 and 55 cm (± standard deviation) from select sites. Site 5 BSi is averaged for 0-30 cm.

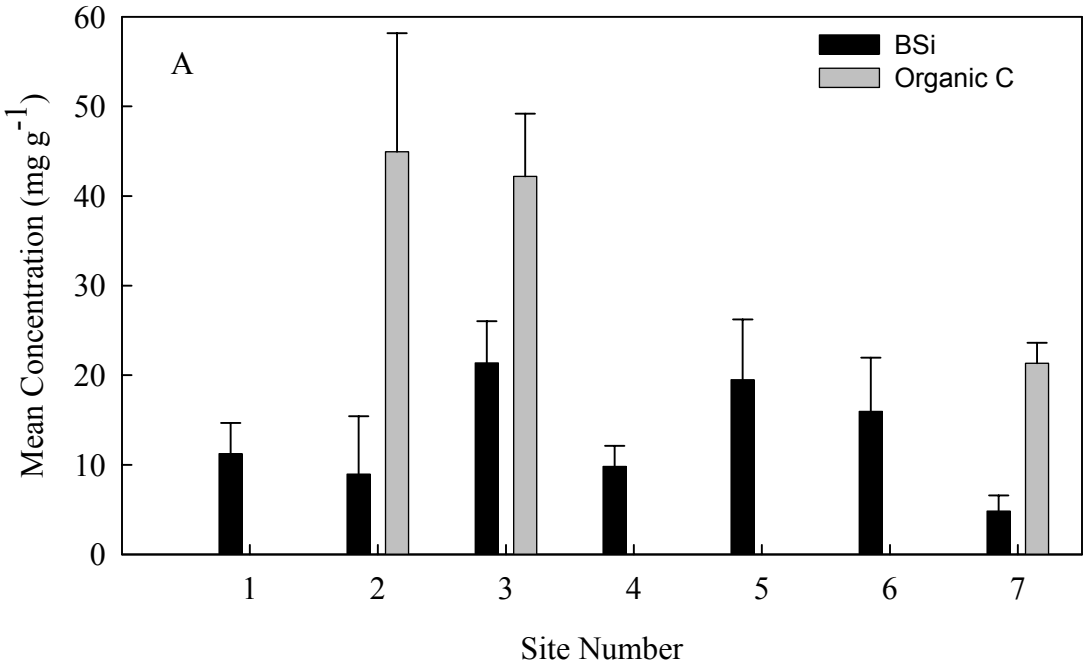

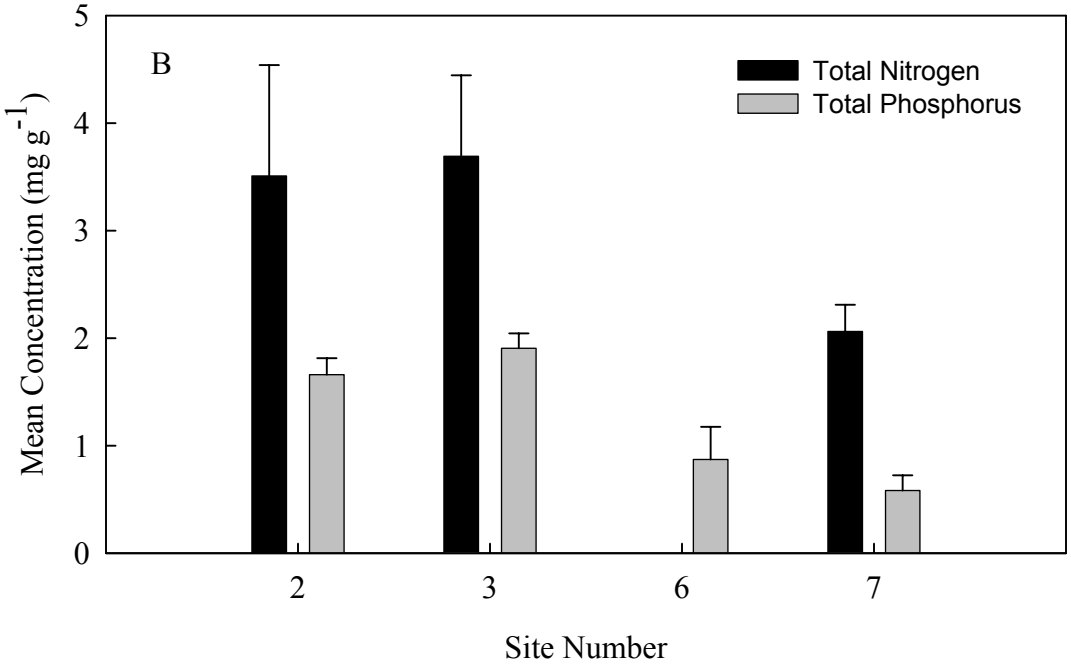

CHAPTER TWO

IRON SULFIDE MINERAL GEOCHEMISTRY AND THE DISTRIBUTION OF SEDIMENT INORGANIC PHOSPHORUS ACROSS AN ESTUARINE SALINITY GRADIENT

ABSTRACT

Although salinity and redox gradients are defining features of estuarine biogeochemistry, compositional changes in sediment characteristics associated with these factors are poorly described in U.S. coastal plain estuaries. To determine the effect of salinity on sediment sequestration of P, sediment cores (30 cm ≤ length ≤ 103 cm) were collected from 7 stations within an oligohaline to mesohaline transect of the Patuxent River estuary. Burial rates of Fe and inorganic P (IP) were greater in oligohaline areas of the estuary than in mesohaline areas. Degree of pyritization (DOP) ranged between 0.04 and 0.31 and generally increased with increasing salinity. DOP values indicated pyrite formation was limited by S availability at oligohaline sites and Fe availability at mesohaline sites. Sedimentary Fe-oxide concentrations were positively correlated with IP concentrations while pyrite and IP were negatively correlated. Thus the formation of pyrite, mainly in mesohaline sediments, limited the availability of Fe-oxides for adsorption and retention of IP.

INTRODUCTION

Estuarine environments, by virtue of their location at the freshwater-marine interface, often encompass a distinct salinity gradient. Characteristic salinity regimes vary from freshwater sources to estuary mouth; salinity within an estuarine zone may also vary seasonally and inter-annually depending on precipitation and flow conditions. Both nutrient cycling and redox chemistry are strongly affected by the salinity gradient.

The large scale effects of cultural eutrophication on coastal systems (Nixon 1995, Cloern 2001, Kemp et al. 2005) have stimulated considerable research effort on characterizing nutrient dynamics and the response of ecosystems to increased nutrient inputs. In order to mitigate the effects of cultural eutrophication, it is necessary to understand the mechanisms controlling nutrient availability and sequestration within the estuary. Therefore, investigations of sediment composition must be made within the context of salinity and redox conditions, defining features of estuarine biogeochemistry. Sediment nutrient interactions, specifically the influence of Fe and S processes on long-term nutrient burial within the estuary, require more detailed study.

Characteristic differences in biogeochemistry among tidal freshwater, oligohaline and mesohaline systems have significant effects on nutrient cycling and burial within an estuary. A number of redox reactions affected by salinity (Table 2.1) occur within these different salinity regimes. In many freshwater environments, P is bound to Fe-oxides and is efficiently sequestered in sediments. In aquatic environments influenced by salinity, P may be released from sediments following Fe and sulfate reduction and the subsequent formation of iron-sulfide minerals. Indeed, Caraco *et al.* (1990) have described greater P release (relative to bottom water metabolism) from brackish/marine systems than from freshwater systems. Sedimentary profiles from the Patuxent River indicate phosphorus

accumulation decreases with increasing distance from the head of the estuary (Jordan et al. *In Press*).

Iron-Sulfur Mineral Forms and their Environmental Significance

The degree to which Fe and S chemistry may influence sedimentary P release is dependent upon the stability of the Fe-S minerals formed after diagenesis. Two Fe-S mineral phases discussed in this paper, iron monosulfides (FeS) and pyrite (FeS_2) have been defined operationally by their respective extraction procedures. Berner (1964) defines acid volatile sulfides (AVS) as those sulfur species that may be volatilized to H_2S upon addition of 1N HCl. Sulfur species that may be extracted with this technique include solid phase Fe-S minerals (amorphous-FeS: mackinawite and greigite; and a fraction of the pyrite pool: FeS_2) as well as dissolved species contained in sedimentary pore water (S(-II), FeS clusters, FeS nanoparticles; Rickard and Morse 2005). For most field studies the assumption that AVS is dominated by the amorphous-FeS pool is acceptable (Cornwell and Morse 1987); the terms AVS and FeS have been used interchangeably for the purposes of this paper. Similarly, chromium reducible sulfur (CRS) is composed mainly of FeS_2 (pyrite) and elemental sulfur (Canfield et al. 1986). Elemental sulfur is usually a small component of CRS (Morse and Cornwell 1987); thus the terms CRS and pyrite are often used interchangeably as well.

Iron monosulfide minerals (FeS) are a common precursor to pyrite (FeS_2) formation (Gagnon 1995), and they are thermodynamically less stable than FeS_2 (Lord and Church 1983, Morse and Cornwell 1987). Thus, FeS_2 represents a more permanent form for sedimentary Fe burial. The permanent burial of Fe via FeS_2 formation may limit the burial of phosphorus, thus allowing for the release of dissolved inorganic P from

sediments. Rozan *et al.* (2002) observed seasonal correlations between Fe-S-P cycling in a temperate estuary (Rehoboth Bay, Delaware) indicating Fe redox chemistry to be a major control of P flux from sediments to overlying water; specifically, P was released from sediments only during periods of solid FeS/FeS_2 production (summer).

Differences in Fe cycling and sedimentary P retention among salinity regimes may be one explanation for differences in nutrient limitation in fresh and marine environments (Caraco et al. 1990; Blomqvist et al. 2004; Jordan et al. *In Press*). Relative availabilities of N and P can select for domination by different primary producers (Howarth and Marino 2006). Therefore, increased P concentrations (attributed to sedimentary P release following Fe-S mineral formation) may influence species composition by lowering the N: P ratio in salinity affected areas. This phenomenon may be exacerbated by eutrophication as increased nutrient concentrations lead to increased organic C deposition and greater reducing conditions in sediments (Howarth and Marino 2006) thus creating a positive feedback of greater P release and lower N: P ratios. Iron and S interactions may directly influence P cycling; however, these and other redox reactions may also indirectly influence N cycling through associated feedbacks in P cycling and primary production (e.g. Kemp et al. 2005; Jordan et al. *In Press*).

Indices of Iron-Sulfur Mineral Formation: DOP and $FeS:FeS_2$

The degree of pyrite accumulation has been used as an indicator for a number of paleo-environmental conditions. Berner *et al.* (1979) observed $FeS: FeS_2$ ratios >10 in marine sediments and ratios < 1 in freshwater sediments; he suggested that general paleo-salinity for a given area may be reflected by the Fe-S minerals formed during sediment burial. Raiswell *et al.* (1988) utilized the degree of pyritization (DOP) as a paleo-

environmental indicator of bottom-water oxygenation (aerobic: DOP < 0.46; dysoxic: 0.46<DOP<0.75 dysoxic; euxinic: DOP >0.75). DOP is defined as (Berner 1970):

$$DOP = \text{Pyrite-Fe}/(\text{pyrite-Fe} + \text{HCl-Fe})$$

Arguably, DOP may have limited applications in describing the reactivity of Fe and as an index for comparing different ecosystems (Canfield et al. 1992); however, site comparisons within a single system can help define changes in iron sulfide mineral formation associated with changes in biogeochemical characteristics such as salinity, redox conditions, and degree of organic matter loading (Cornwell and Sampou 1995). Pyrite formation may be influenced by three major factors: 1) Fe availability 2) S availability (mainly as sulfate) and 3) organic matter loading to the sediments (Berner 1970). Sediment mass accumulation rates also play an important role in the delivery of organic matter and iron. For example, greater sediment accumulation rates may be associated with greater deposition of organic matter and iron; thus, sediment accumulation rates may indirectly influence pyrite formation.

Characterizing Iron-Sulfur Mineral Formations in Estuarine Salinity Transition Zones

Previous studies investigating sedimentary pyrite formation and inorganic P release have focused on biogeochemical dynamics in the upper sediment profile (i.e. within the zone of active redox cycling) while studies describing Fe and S accumulation have examined sedimentary profiles for signals of anthropogenic impacts on the estuary. Several studies of long sediment cores collected from the mesohaline portion of Chesapeake Bay describe an increase in sediment sulfur concentrations since the mid-20th century. Greater DOP values, associated with the increased incidence of reducing

conditions and bottom water hypoxia/anoxia, correspond to increases in terrestrially derived nutrient inputs to the estuary (Cornwell and Sampou 1995, Cooper and Brush 1991). Zimmerman and Canuel (2000) describe a near 2-fold increase between 1934 and 1948 in organic carbon and total sulfur in sediment profiles, coinciding with an increase in the sediment AVS/CRS (associated with greater AVS storage); these factors indicate that greater reducing conditions in bottom waters of this region are associated with greater organic matter delivery during this period (Zimmerman and Canuel 2002). However, most investigations of changes in FeS and FeS_2 burial have been limited to areas with extensive pyrite formation (i.e. mesohaline and polyhaline areas not limited by sulfate availability). Given the known influence of organic matter loading on sulfate reduction (Roden and Tuttle 1993) and pyrite formation, investigations regarding Fe-S mineral formations must not be limited to mesohaline areas alone, but should include regions of high productivity such as estuarine salinity transition zones.

Estuarine salinity transition zones are characterized by shifting redox conditions, dynamic nutrient cycling, and intensive primary productivity (Kemp and Boynton 1984, Capone and Kiene 1988, Roden and Tuttle 1993); however, few studies have attempted to investigate the burial of Fe-S minerals within the context of this estuarine gradient. In order to determine the effect of salinity and redox status on nutrient burial, I analyzed sedimentary profiles of phosphorus, iron, and sulfur species collected from sediment cores at seven sites within the salinity transition zone of the Patuxent River estuary, a tributary of Chesapeake Bay. Nutrient inputs and transformations within this estuary are well documented (Boynton et al. 1995, Jordan et al. 2003, Fisher et al. 2006). Jordan *et al.* (*In Press*) have described porewater Fe biogeochemical distributions as having higher

concentrations at freshwater sites than at saline sites; phosphate and sulfate concentrations were greater at mesohaline sites. These findings suggested that Fe-S dynamics may influence differences in P cycling and thus nutrient limitation within the salinity transition zone of the Patuxent River. However, determination of the distributions of sedimentary Fe-S mineral accumulation in the salinity transition is required to define the relationship between sedimentary inorganic phosphorus and Fe-S mineral formation.

METHODS

Study Site

The study area focuses on the salinity transect of the upper tidal Patuxent River estuary (Fig. 2-1). The 2,393 km^2 watershed of the Patuxent River is located entirely in the state of Maryland, USA; dominant land uses are forests and medium density residential development (MDP 2000). Seven coring locations were chosen with salinities ranging from freshwater to mesohaline (salinity of 4-14). Water column depths in the study area were, on average, less than 7 m. Although deeper waters of the lower estuary may experience stratification and hypoxia, fresh and oligohaline waters are vertically well mixed and aerobic (Lung and Bai 2003; Hagy et al. 2000) as are the shallow sub-tidal areas chosen for mesohaline core collection in this study. In general, sediment grain size is dominated by silt and clay (Cornwell unpublished data).

Sample Collection and Preparation

Sediment cores (30 cm < core length < 105 cm) were collected in June and August 2004 from seven shallow (water column depth < 7 m) sub-tidal locations

encompassing the salinity transition zone of the Patuxent River estuary (Table 2-2). Sediment cores were collected in summer to correspond with maximum sulfate reduction rates (e.g. Roden and Tuttle 1993). Cores were collected using a hand-deployed piston corer (8 cm inner diameter; Abysmal Corers, Colorado). Cores were transported to the laboratory and sectioned within 24 hours of collection. Sediment section intervals were 1.0 cm (0-10 cm depths), 2.0 cm (10-30 cm depths), 5.0 cm (30-60 cm depths), or 10.0 cm (60-100 cm depths). Sediments were homogenized in polypropylene beakers; sub-samples from each section (approximately 10 mL wet volume) were stored in polyethylene snap-cap vials and frozen for acid volatile sulfur (AVS) analysis; the remaining sediment was placed in aluminum pans and dried in a forced-air oven at 80°C. Sediment samples were dried to a constant weight, ground by hand (using a porcelain mortar and pestle), and stored in plastic bags at room temperature for further analysis.

Geochemical Analysis

Inorganic phosphorus was extracted from sediment using 1N HCl (Aspila et al. 1976) and analyzed colorimetrically following the molybdenum blue technique of Parsons *et al.* (1984). The HCl extracts were also used to determine the concentration of HCl-extractable Fe on a flame atomic absorption spectrophotometer (Leventhal and Taylor 1990). Acid volatile sulfide (AVS) was analyzed from frozen sub-samples using 6N HCl volatilization; $SnCl_2$ was not added to avoid extraction of pyrite-S in the AVS pool (e.g. Cornwell and Morse 1987). Chromium reducible sulfur (CRS) was extracted from dry sediment following Canfield *et al.* (1986); dry sediments produce similar results to samples analyzed without drying (Morse and Cornwell 1987). Iron-oxide (FeOOH)

concentrations were determined to be equal to HCl-Fe minus AVS-Fe (assuming AVS = FeS).

RESULTS

Description of Fe Accumulation within the Patuxent River Salinity Gradient

Iron oxides were the dominant Fe pool at all sites within the Patuxent River salinity transition zone (Fig. 2-2). AVS-Fe was minimal at all sites and CRS-Fe importance increased at sites 4, 5, 6, and 7. At site 7, iron oxides dominated the surface and sub-surface sedimentary Fe pool; however, concentrations of CRS-Fe and Fe-oxides were approximately equal at depths > 30 cm. A similar trend was observed in site 6 sedimentary profiles. The CRS-Fe profile from site 4 indicated peaks of pyrite formation between 15 and 40 cm with lower concentrations at greater depths.

An increase in CRS-Fe between 15 and 40 cm and decrease at depth may arise from two different mechanisms:

1) Historic sediments, characterized by greater Fe-oxide concentrations (below 40 cm at site 4), accumulated during periods of greater freshwater inputs; or,

2) Pyrite is formed at mid-depths and re-oxidized in deeper sediment sections.

This phenomenon of peak pyrite accumulation at sediment depths less than peak Fe-oxide accumulation was not observed in other cores collected for this study. Peak pyrite accumulation in other cores occurred at depths where Fe-oxide concentrations were decreasing or stabilized. It is unclear why site 4 varied from this typical characterization. Sediment dating was not successful at site 4 (Chapter 1), so it is unclear if differences in mass accumulation rate may be contributing to this observed anomaly. The possible

influence of changes in freshwater flow will be discussed later in this paper; however, it is important to note that because site 4 is adjacent to a marsh with a tidal creek, it is possible that localized perturbations in flow may influence sediment redox dynamics at this site in a unique manner.

Indices of Fe-S Mineral Formation

Within the salinity transition zone of the Patuxent River, mean DOP values ranged between 0.04 and 0.31 (Fig. 2.3A). Of the seven sites, the three upper estuarine sites (1: tidal freshwater, 2 and 3: oligohaline) had the same mean DOP value (0.04 ± 0.02). Mean DOP values increased with increasing distance from the head of the estuary; mean DOP values from sites 4, 6, and 7 were more than 15 times greater than mean DOP values at sites 1, 2 and 3 (Fig. 2.3A).

Variability in DOP with depth also increased with increasing salinity. Profiles of sites 1, 2, and 3 revealed consistent DOP values throughout sampled sediment cores (Fig. 2.4), whereas sites 5, 6, and 7 were generally characterized by increasing DOP values with sediment depth (Fig. 2.4). In all sediment cores peak DOP values occurred at depths >29 cm (Fig. 2.4). Although the mean DOP value at site 4 was more similar to the lower estuarine sites (Fig. 2.3A), the sedimentary profile of DOP at site 4 was variable. Similar to sites 5, 6, and 7, DOP values from site 4 increased between 0 and 35 cm; however below 35 cm, site 4 DOP values abruptly decreased and remained relatively constant below 45 cm (while DOP values at sites 5, 6, and 7 continue to increase or remain constant). Such differences between surface/sub-surface DOP values at site 4 and DOP values at depth may be an indication of recent changes in environmental conditions.

Mean AVS-S: CRS-S ratios were greatest at sites 2 and 3 (Fig. 2.3B). Mean AVS-S: CRS-S ratios > 0.50 indicate sites 2 and 3 preferentially sequestered FeS. Low sulfate availability at site 1 is the likely cause of lower mean AVS-S: CRS-S ratios. Low mean AVS-S: CRS-S ratios at sites 4, 5, 6, and 7 may be the result of rapid AVS conversion to pyrite. Sites 6 and 7 exhibited low yet variable AVS-S: CRS-S ratios between 0 and 30 cm, indicating that resuspension, bioturbation, and redox cycling may influence Fe-S mineral formation through this portion of the sediment profile (Fig. 2.5); however, below 40 cm consistently low (< 0.10) AVS-S: CRS-S ratios indicate pyrite was the preferential mineral form buried in these mesohaline sediments. The profile of AVS-S: CRS-S ratios at site 4 indicate little to no AVS formation in surface and sub-surface sections; however, at depth, AVS-S: CRS-S ratios greater than 0.30 support evidence from DOP values that environmental conditions at this site may have changed in recent decades (Gerritse 1999). The profile of AVS-S: CRS-S ratios from site 2 revealed a distinct outlier at the 35-40 depth interval (Fig. 2.5) which may correspond to an extreme freshwater flow event such as tropical storm Agnes; although initial sediment dating analyses were unsuccessful at this particular site, future analysis of a longer sediment core from this site may be more successful and thus allow for comparisons of known changes in input corresponding with this sediment section (Chapter 1). Although removing this point from the data set would reduce the mean AVS-S: CRS-S ratio to 0.38, this value is still indicative of preferential AVS sequestration.

Mean AVS-S: CRS-S ratios at sites 1, 4, 5, 6, and 7 are less than 0.2 indicating AVS is not preferentially buried in these locations (Fig. 2.3B). DOP values and AVS-S: CRS-S ratios from sites 4, 5, 6, and 7 both give supporting evidence for pyrite formation in

these lower estuarine sites. DOP and AVS-S: CRS-S ratios from site 1 both indicate Fe-S mineral formation is limited in this freshwater site.

Relationship Between IP and Fe-S Minerals in the Patuxent River Salinity Gradient

Average sedimentary inorganic P (IP) concentrations generally decreased with increasing distance from the head of the estuary (Fig. 2.6; also Jordan et al. *In Press*). Site 1 was a notable exception to this trend; average IP concentrations at this site were similar to the mesohaline sites. In the case of this particular location, which appears to have the greatest fluvial influences, grain size may influence the amount of sorbed-P in accumulated sediments (Jordan et al. *In Press*).

Inorganic phosphorus and Fe-oxides were positively correlated ($p \leq 0.01$; Fig. 2.6) at all sites except site 2 (no correlation); inorganic P and pyrite-Fe were negatively correlated ($p \leq 0.10$) at all sites except site 2 where there appeared to be a positive relationship ($p= 0.05$) and site 1 (no correlation). Pyrite-Fe and IP were likely not correlated at site 1 due to the small amount of pyrite formation at this oligohaline site. Despite a broad range of Fe-oxide concentrations (200-600 μmol g^{-1}) throughout the sediment core profile from site 2, Fe and inorganic P concentrations were not significantly correlated; however, inorganic P concentrations increased with increasing pyrite-Fe concentrations at site 2 ($p<0.01$). Outliers were omitted from the final correlation analysis of site 4 (n=1) and site 6 (n=3). These outliers were attributed to IP concentrations that were uncharacteristically high in comparison to IP concentrations in the rest of the sediment core; it is possible that these outliers are related to uncharacteristic flow events, bioturbation, or are associated with experimental error.

DISCUSSION

Characterizing Sedimentary Fe and P Accumulation in the Patuxent River Estuary Salinity Transition Zone

In the salinity transition zone of the Patuxent River, Fe-oxides dominated the Fe pool; however, pyrite became a more important component of the Fe pool at more saline sites in this study. Pyrite formation was correlated with decreased inorganic P concentrations at all sites but the tidal freshwater site. Degree of pyritization calculations indicated that pyrite formation was limited by iron availability in mesohaline sediments while sulfur availability was limiting in oligohaline sediments. These findings are similar to those of other studies examining sediments from tidal freshwater and brackish marshes (Hyacinthe and Van Cappellen 2004). However, this study adds further understanding to estuarine Fe-S-P dynamics by characterizing Fe-species along the salinity continuum.

Additionally, this study captures the importance of sedimentation rate on differential accumulation of Fe within a salinity gradient as well as the ramifications of this differential accumulation for Fe-S mineral formation and sedimentary P accumulation. Differences in organic matter loading to sites in the middle salinity transition zone, due to 1) differences in mass accumulation rate or 2) differences in primary productivity, may influence sedimentary sulfate reduction rates and thus influence the availability of S for pyrite formation. Greater organic matter production and deposition as well as enhanced sulfate reduction rates in the mid-salinity transition zones of estuaries have been documented by several studies (Kemp and Boynton 1984; Capone and Kiene 1988; Roden and Tuttle 1993). Additionally, Westrich and Berner (1984) observed that sulfate reduction is directly proportional to the concentration of metabolizable organic carbon. Thus, as Howarth (1984) concluded, the contribution of

sulfate reduction to carbon remineralization is greatest in highly productive environments, such as shallow sub-tidal sediments.

Such a characterization typifies the Patuxent River salinity gradient and even more specifically exemplifies sites located in the mid-salinity transition zone (sites 3, 4, and 5 in this study). Along the Patuxent River salinity gradient, total Fe concentrations (HCl-Fe plus CRS-Fe), were greatest at site 3. Sediment accumulation rates at this site were more than 10 times greater than sedimentation rates determined for other sites in this study (Chapter 1). Although sedimentary Fe concentrations were not 10 times greater than other sites, the greater Fe pool at site 3 is likely the result of greater sediment accumulation. Fe-S mineral formation in locations of high sedimentation may be enhanced by this relationship between sedimentation rate and Fe delivery. Additionally, sedimentary carbon content was greater at site 3 than at site 7 (Chapter 1). Therefore, this location is receiving greater inputs of carbon and organic matter than the other locations studied. Greater inputs of labile carbon would require greater sedimentary oxygen demand thus decreasing the redox potential leading to enhanced sulfate reduction (compared with other study locations with less organic matter inputs).

Environmental Influences on Fe-S Mineral Formation and Sedimentary P Retention

Profiles of sedimentary pyrite accumulation indicated a historical difference in Fe-S mineral formation at site 4 which may be indicative of changes in environmental conditions. Although site 4 DOP values between 0 and ~ 40 cm were generally similar to DOP values of the mesohaline study sites (6 and 7), DOP values between 40 and 60 cm approached those of oligohaline study sites (Fig. 2.4). Lower DOP values in deeper

sediment sections may be associated with lower salinity conditions in previous decades or less organic matter deposition. Because sediment dating techniques were unsuccessful at this particular site (Chapter 1), it is unclear if historical differences in mass accumulation rates (and thus differences in organic matter loading; e.g. Berner 1970) or historical differences in salinity (e.g. Berner et al. 1979) may have contributed to this observation. It must be noted that site 4 was located adjacent to a tidal creek (Summerville Creek) and thus may experience more variability than other study locations due to its proximity to terrestrial inputs. However, alterations in freshwater flow (due to changes in land-use, freshwater withdraw within the watershed, and global climate) may have important consequences for Fe-S mineral formation within the entire salinity transition zone.

In the Patuxent River estuary salinity transition zone the formation of Fe-S minerals was more prominent in areas with greater mean salinity. In a given year, the amount of freshwater flow from the watershed is an important factor controlling the extent of salinity intrusion up the estuary (Hagy et al. 2000). The amount of freshwater flow is influenced by precipitation in the watershed and reservoir management for drinking water (Weller et al. 2003). Despite some inconsistencies and difficulties in predicting future precipitation in the Mid-Atlantic region, most climate change models agree that both winter and spring will become wetter in the coming years and overall mean temperature will increase (Najjar 1999). Increases in temperature will likely increase evapotranspiration during peak growing seasons. Thus climate change may lead to decreased freshwater flow during summer months, corresponding to peak periods of sulfate reduction. Within the Patuxent River estuary, this may result in salinity intrusion

further up the estuary thus providing a larger area for sulfate reduction, Fe-S mineral formation, and sedimentary P release.

Future changes in land-use may also influence freshwater flow. Land-use in the Patuxent River estuary watershed is currently dominated by forest and grassland; however, with increasing development in this region it is expected that more of the watershed will be characterized by developed land-uses with the potential for greater nutrient discharges from point sources. Although improvements in wastewater treatment have reduced nutrient concentrations in wastewater discharges, volumes of discharges from the largest treatment plants in the watershed are still increasing (Sprague et al. 2000) increased water flow from developed land would be the likely result from increased impervious surfaces preventing absorption of water within the watershed as well as from decreased evapotranspiration following land clearing (Weller et al. 2003). Increased development within the watershed may also lead to reduced water discharge as increasing populations place increased demand on reservoir water sources.

Given the history of water use in the Patuxent River watershed and predicted discharges to the Patuxent River estuary in the future, it is likely that freshwater flow during summer months will be reduced. Decreased freshwater flow may allow for salt-water to intrude further up estuary. Areas currently characterized by oligohaline conditions may experience greater salinity in summer months thus allowing for greater sulfate reduction to occur (Weston et al. 2006). Such conditions would enhance Fe-S mineral formation and may lead to increased sedimentary P release from areas that previously acted as P-sinks (Canavan and Slomp In Prep.).

Implications of Differential P Retention and Fe-S Mineral Formation in Estuarine Sediments

On a global scale, Froelich (1988) estimated that fluvial particulates could transport 2-5 times more reactive phosphorus to the sea (1.4-12 x 10^{10} mol yr^{-1}) than the dissolved load alone. En route to the sea, these particles encounter a variety of physical and geochemical environments that may influence P sorption and transport. For example, dramatic gradients in salinity and redox cycling in the upper Patuxent River estuary influence the degree to which pyrite may form in a given area. The presence of pyrite in sediment core profiles may be an indication of a relatively poor efficiency of P retention and/or release of dissolved P.

This newly available dissolved P may play a critical role in nutrient limitation of primary production (Jordan et al. *In Press*). Numerous studies have documented differences between the limitation of primary productivity in freshwater and marine environments. Phosphorus is generally more limiting than nitrogen in freshwater environments, while the reverse situation characterizes marine environments. Although it has been shown that eutrophication of many coastal systems is the result of excess N input (Howarth and Marino 2006), nutrient management strategies targeting only one nutrient species may not be effective. Fisher et al. (2006) documented N limited, P saturated conditions in the Patuxent River resulting from sewage inputs of low N:P (following technological improvements in wastewater treatment). Additionally, sedimentary P retention in estuaries is limited by Fe availability; therefore, greater P inputs, beyond the capacity for efficient Fe-sorption and sedimentary burial, may allow for excess P release to the water column. Such shifts in nutrient content may significantly alter species composition and ecosystem functioning.

CONCLUSIONS

This study focused on characterizing sedimentary Fe-S mineral accumulation in the salinity transition zone of the Patuxent River estuary and examined the relationship between inorganic phosphorus, pyrite, and iron oxides. Findings from this study suggested that, in general, sedimentary pyrite accumulation increased with increasing salinity and that sedimentary inorganic phosphorus was inversely related to pyrite accumulation. The presence of pyrite in these estuarine sediments may be an indication of locations of inorganic phosphorus release. Because peak pyrite formation occurred at sites with the greatest mean salinity, one may conclude that the amount of freshwater discharge from the watershed may influence the location of inorganic phosphorus release resulting from Fe-S mineral formation. Future research investigating Fe-S mineral formation should include measurements of sulfate reduction in order to determine biotic controls on sulfur availability for mineral formation.

Table 2.1 Description of reactions that may influence phosphorus burial in estuarine sediments.

Description Of Reaction	Unbalanced Reaction	Environmental Conditions
Formation of iron oxides and adsorption to phosphate*	PO_4^{3-}+Fe(II) → Fe(III)OxPO_4	Aerobic
Iron (III) reduction**	Fe(III)OxPO_4 → PO_4^{3-}+Fe(II)	Anaerobic
Sulfate reduction**	SO_4^{2-} → S^-	Anaerobic, saline
Pyrite formation**	Fe(II) + S^- → FeS_2	Anaerobic, saline

*Source: Cornwell 1987
**Source: Krom and Berner 1980

Table 2.2 Description of sub-tidal sediment cores collected in the salinity transition zone of the Patuxent River and relevant collection site physical characteristics.

Site Number	Date Collected	Coordinates	Salinity*	Core Length (cm)	Water Column Depth** (m)	Water Content (%)	Ash Free Dry Weight†	Sediment Mass Accumulation Rate††
1	8/23/2004	38°46.130'N 76°41.967'W	0-0	63	1.0	29 - 55	3.75 ± 4.06	n/a
2	6/21/2004	38°41.120'N 76°41.537'W	0-1	93	1.6	58 - 81	15.3 ± 1.71	n/a
3	6/21/2004	38°37.677'N 76°40.689'W	0-3	103	1.4	62 - 85	12.2 ± 0.25	18,105
4	8/23/2004	38°35.434'N 76°40.316'W	0-4	68	1.5	45 - 64	5.16 ± 0.55	n/a
5	8/23/2004	38°33.520'N 76°40.283'W	1-5	30	1.5	70 - 82	12.3± 0.83	n/a
6	8/23/2004	38°31.043'N 76°39.778'W	1-8	56	6.0	64 - 79	10.8± 0.73	1831
7	6/21/2004	38°29.313'N 76°40.052'W	3-11	77	2.4	61 - 75	9.25 ± 0.33	2183

*Range of the average March through August salinity as monitored by the Chesapeake Bay Program (1990-1998; as reported in Jordan et al. In Press). **Water column depth at time of core collection; average water column depths may vary according to tides. †Ash-free dry weight was averaged for the top 5 cm of each sediment core. ††Units are g m^{-2} y^{-1}.

Figure 2.1 Map from Jordan et al. (I*n Press*). Left: The Patuxent River Estuary and its watershed. Right: Enlargement of the upper estuary (30-70 km from the mouth) showing the seven sampling sites.

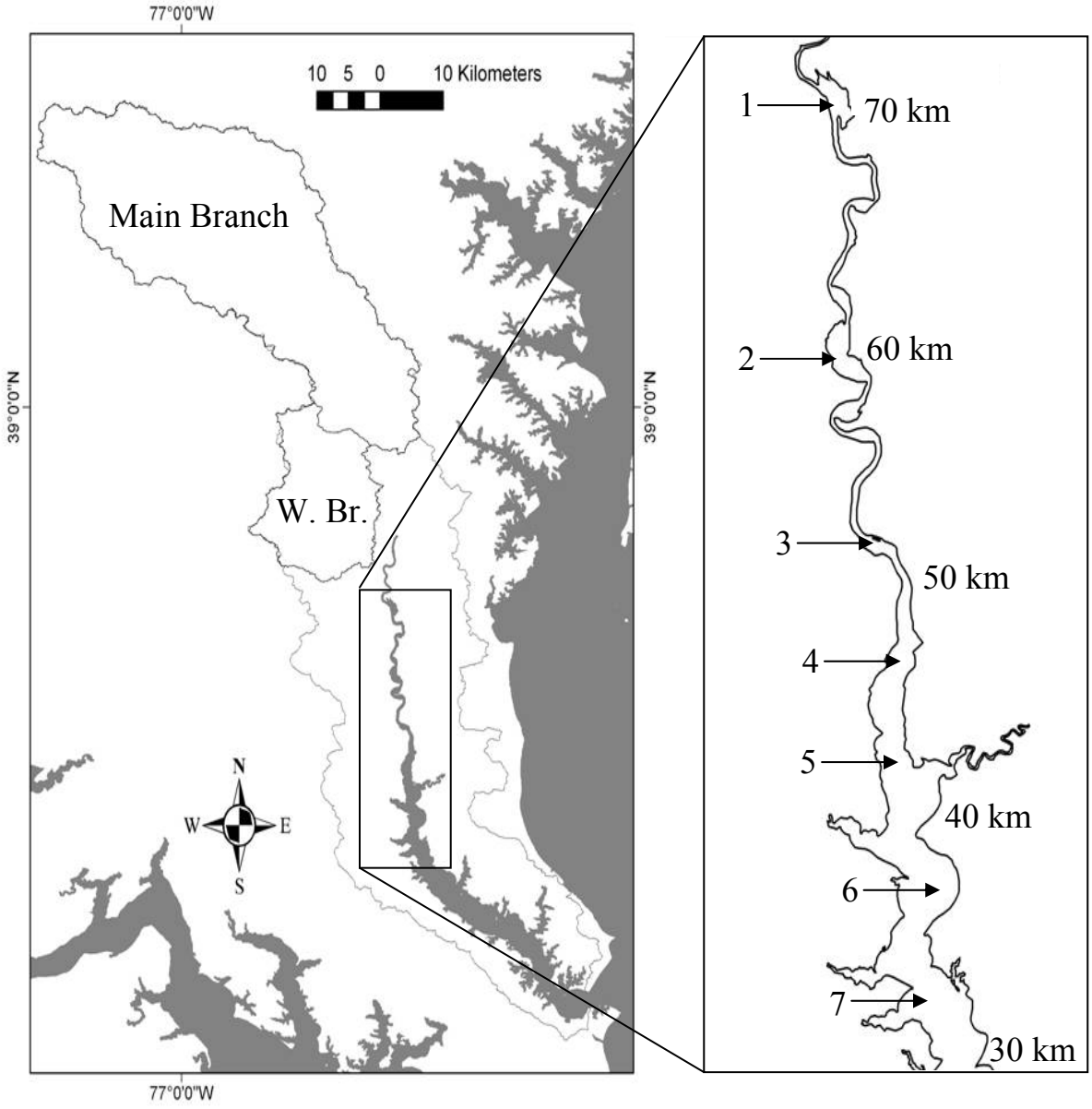

Figure 2.2 Sedimentary profiles of FeS, Pyrite-Fe, and Fe-oxides from 7 sites within the Patuxent River salinity gradient.

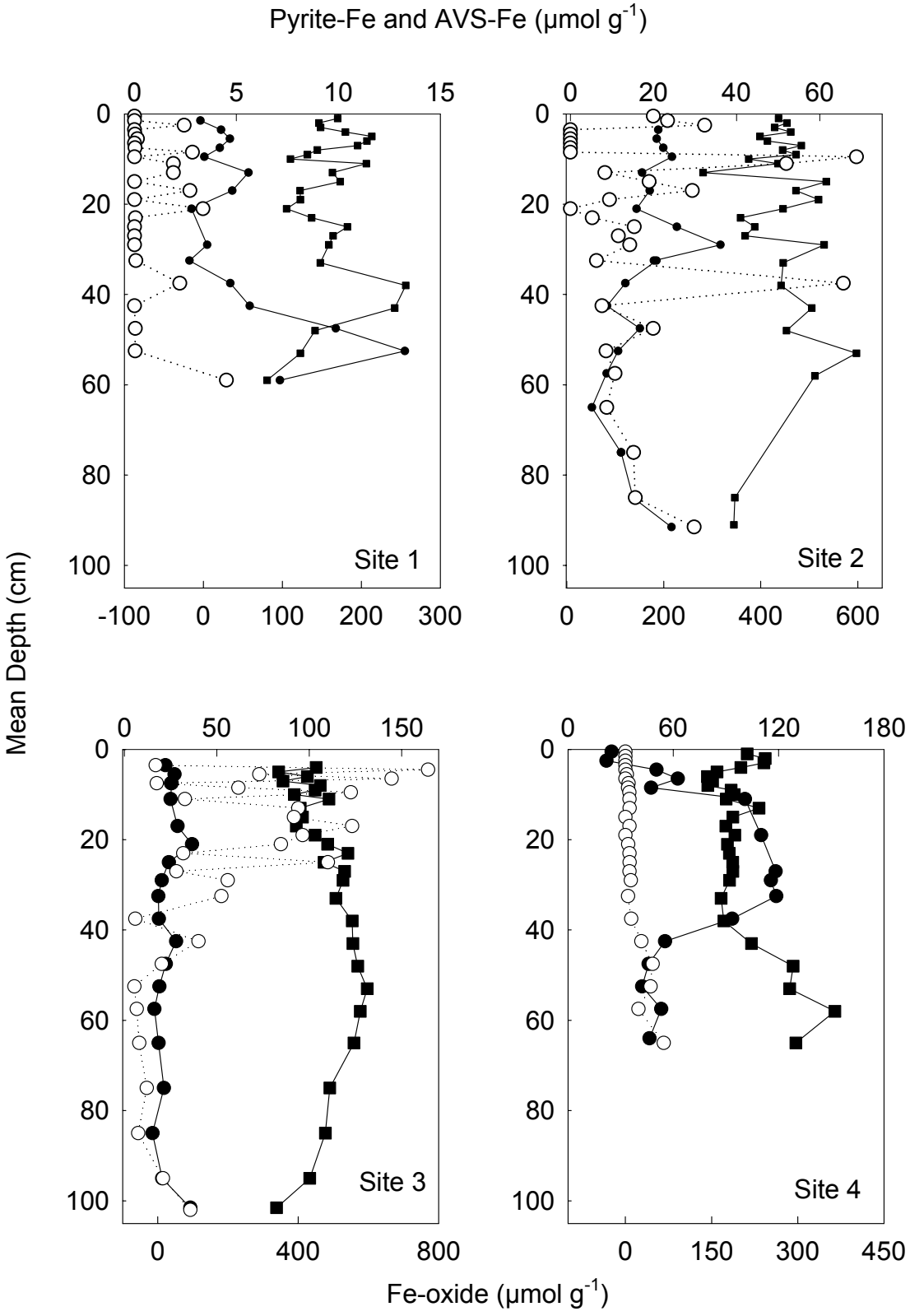

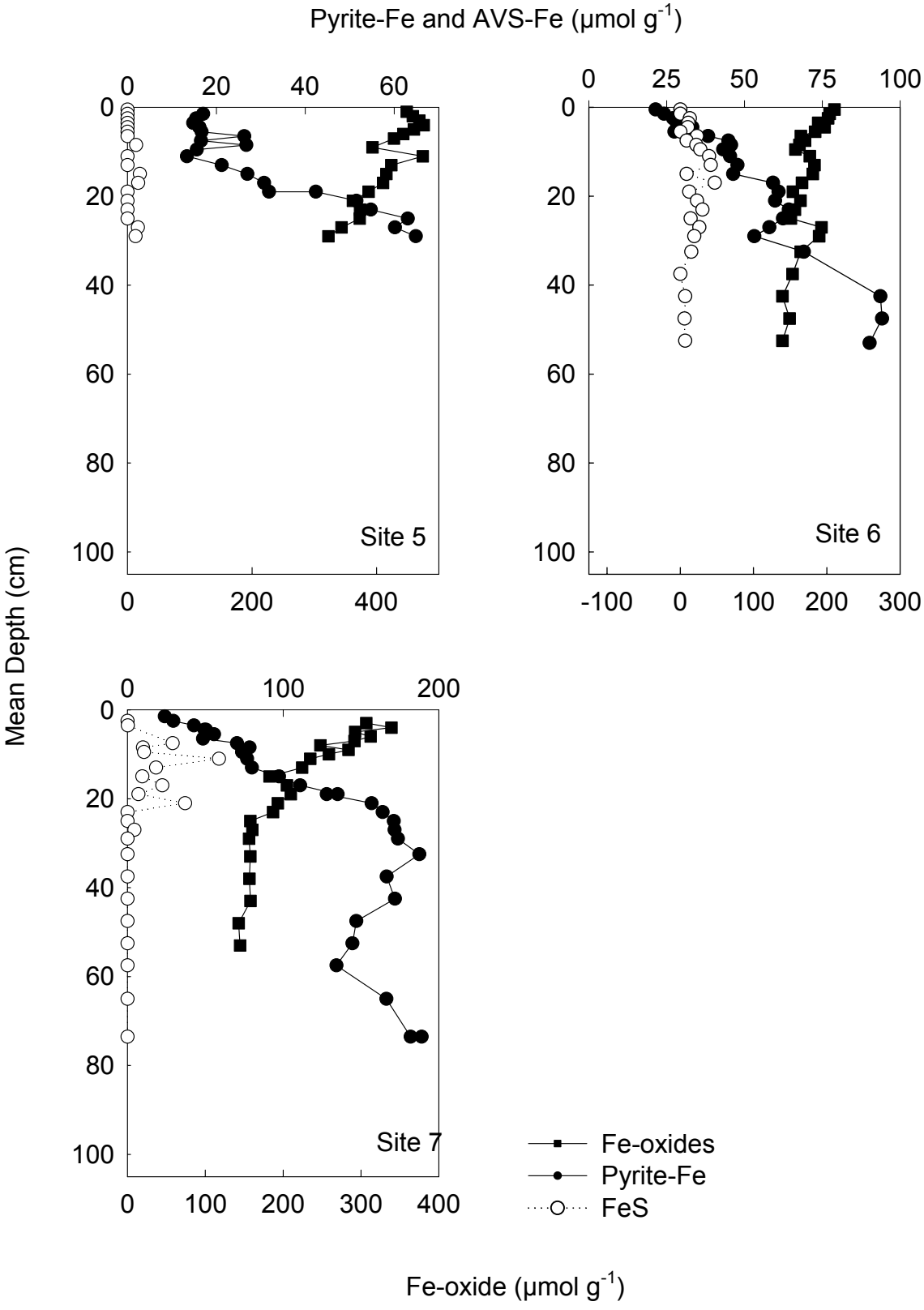
Pyrite-Fe and AVS-Fe (µmol g-1)
Mean Depth (cm)
Fe-oxide (µmol g-1)
Site 5
Site 6
Site 7
Fe-oxides
Pyrite-Fe
FeS

Figure 2.3 Mean* degree of pyritization (DOP) and mean* AVS-S: CRS-S ratios at seven sites within the Patuxent River salinity gradient.

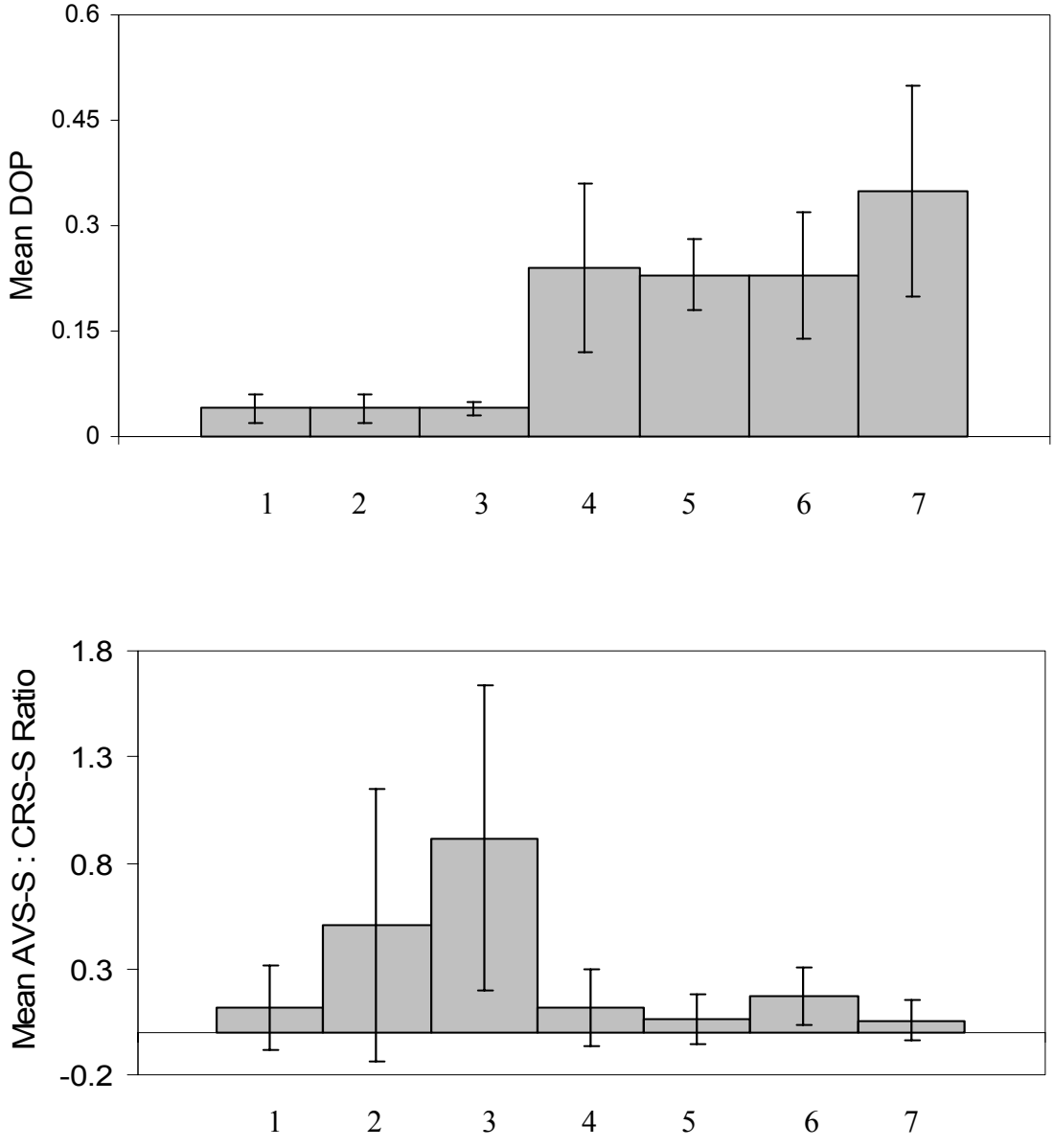

*Mean given for the top 60 cm of each core with the exception of site 5 in which the mean of the top 30 cm is given.

Figure 2.4 Sedimentary profiles of degree of pyritization (DOP) from seven sites in the Patuxent River salinity gradient.

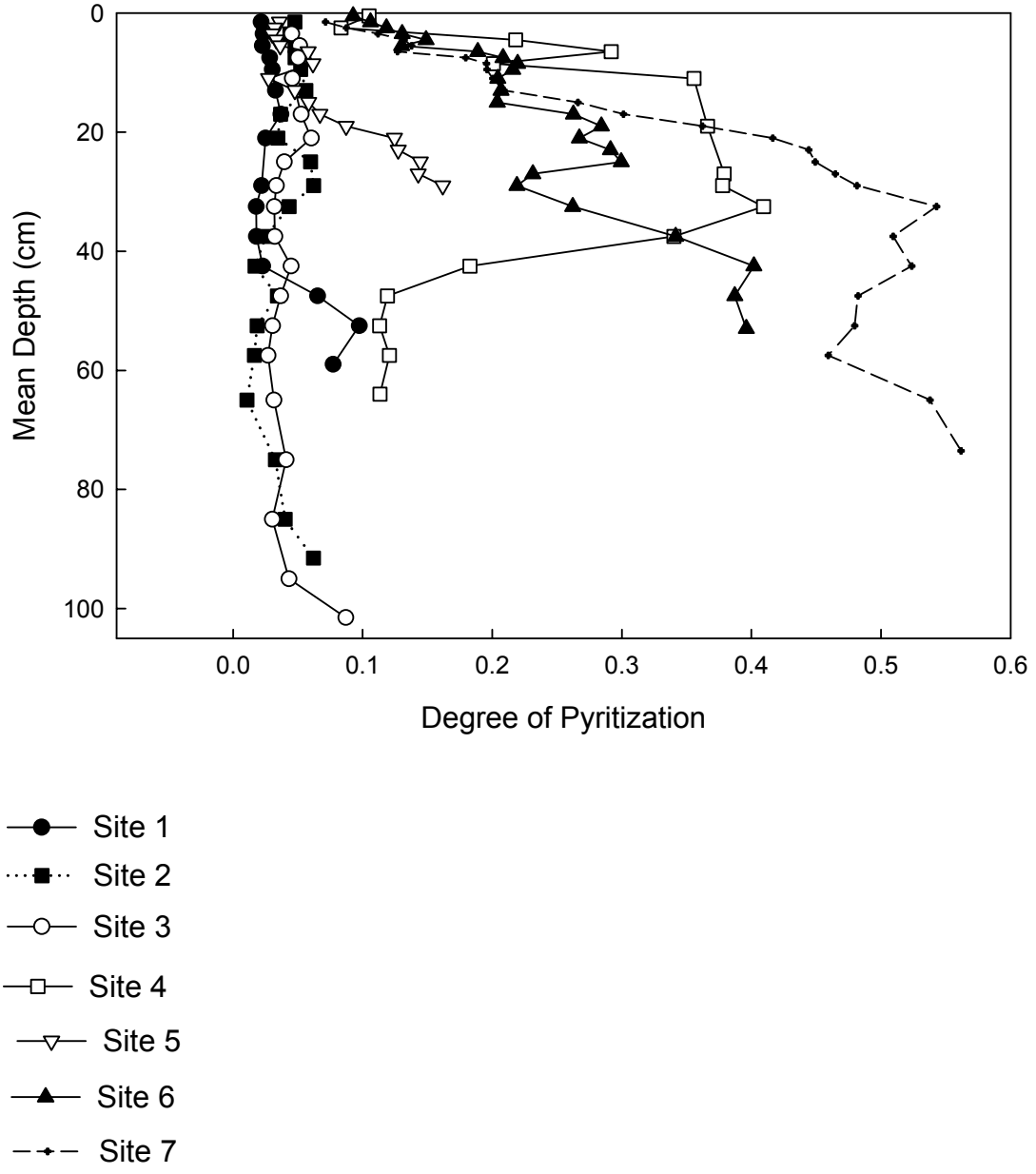

Figure 2.5 Sedimentary profiles of AVS-S: CRS-S ratios from seven sites in the Patuxent River estuary salinity gradient.

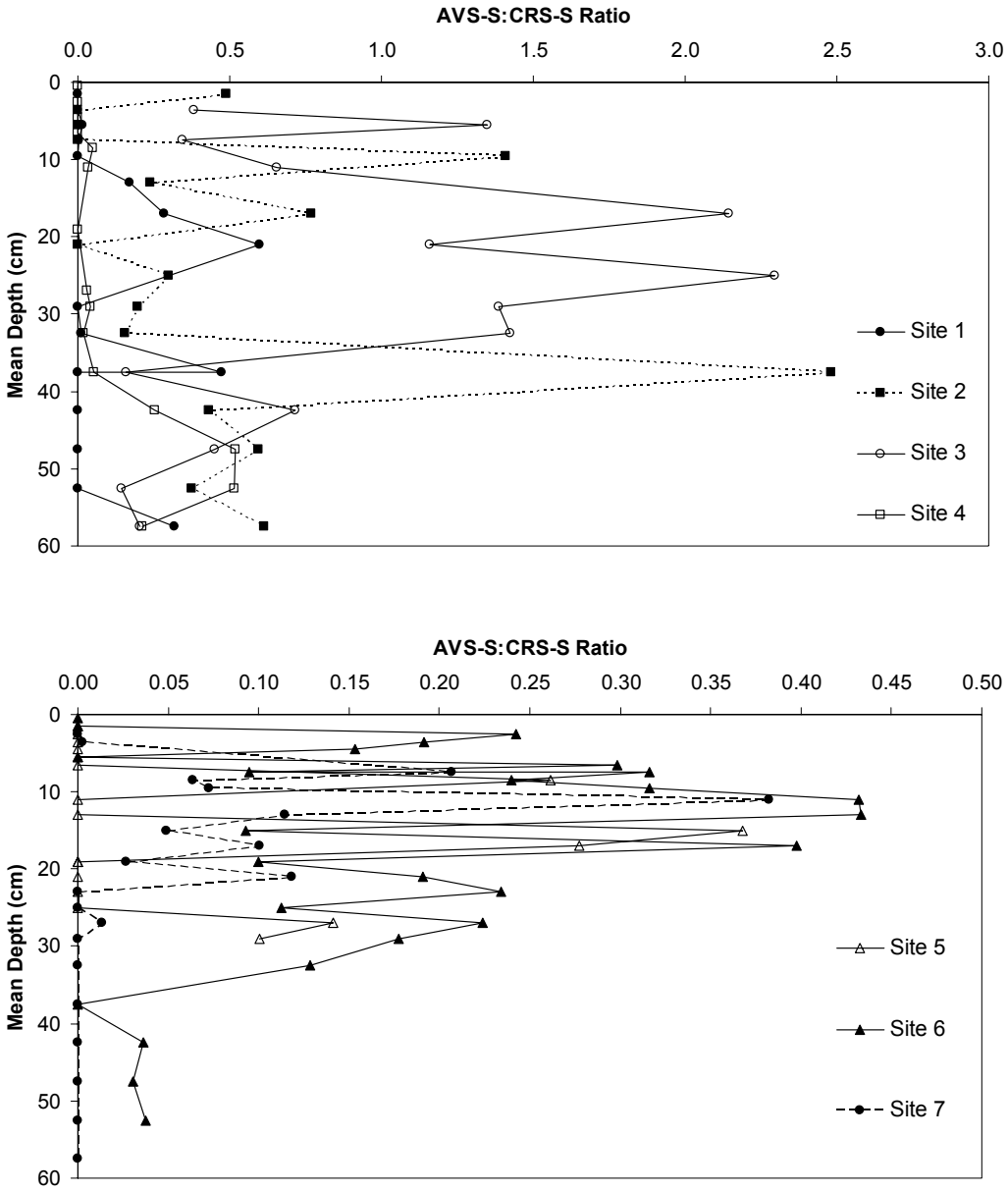

Figure 2.6 Correlations between inorganic phosphorus and HCl-Fe minus AVS-Fe as well as correlations between inorganic phosphorus and pyrite-Fe. Open circles were not included in the final regression; detailed explanation of outliers is provided in the text.

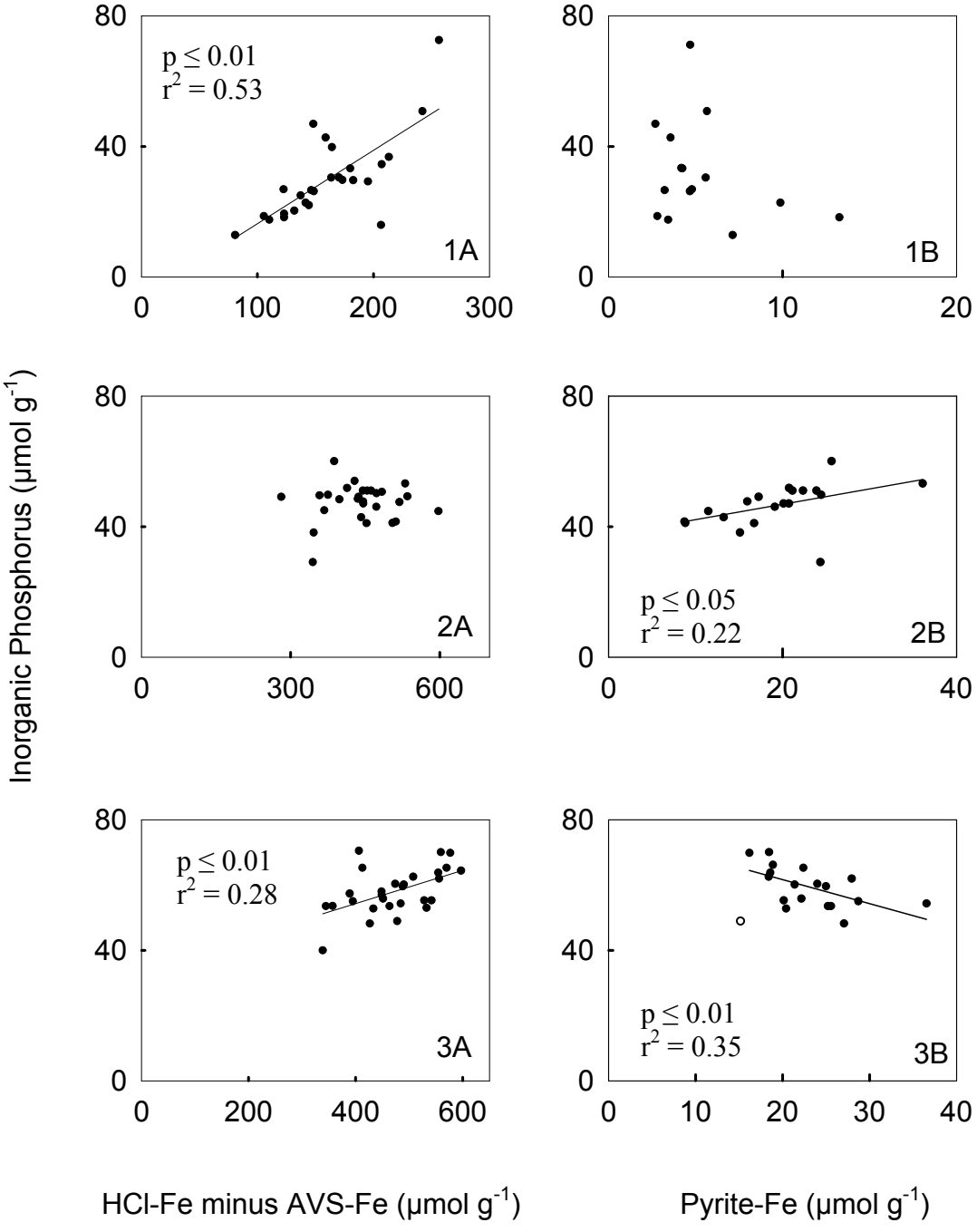

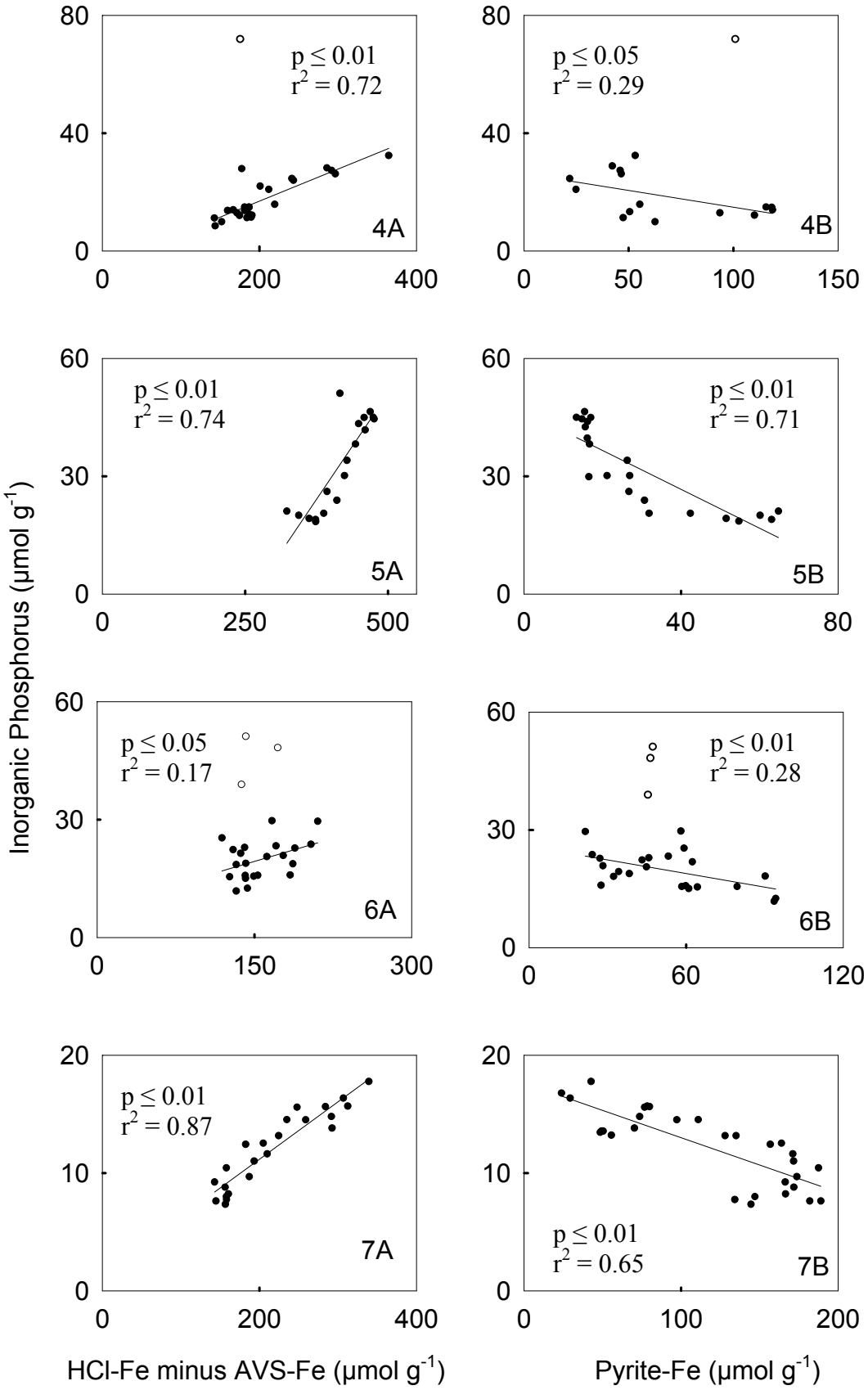
Inorganic Phosphorus (µmol g-1)
p ≤ 0.01
r2 = 0.72
4A
p ≤ 0.05
r2 = 0.29
4B
p ≤ 0.01
r2 = 0.74
5A
p ≤ 0.01
r2 = 0.71
5B
p ≤ 0.05
r2 = 0.17
6A
p ≤ 0.01
r2 = 0.28
6B
p ≤ 0.01
r2 = 0.87
7A
p ≤ 0.01
r2 = 0.65
7B
HCl-Fe minus AVS-Fe (µmol g-1)
Pyrite-Fe (µmol g-1)

Figure 2.7 Sedimentary profiles of inorganic phosphorus concentrations from seven sites in the Patuxent River salinity gradient.

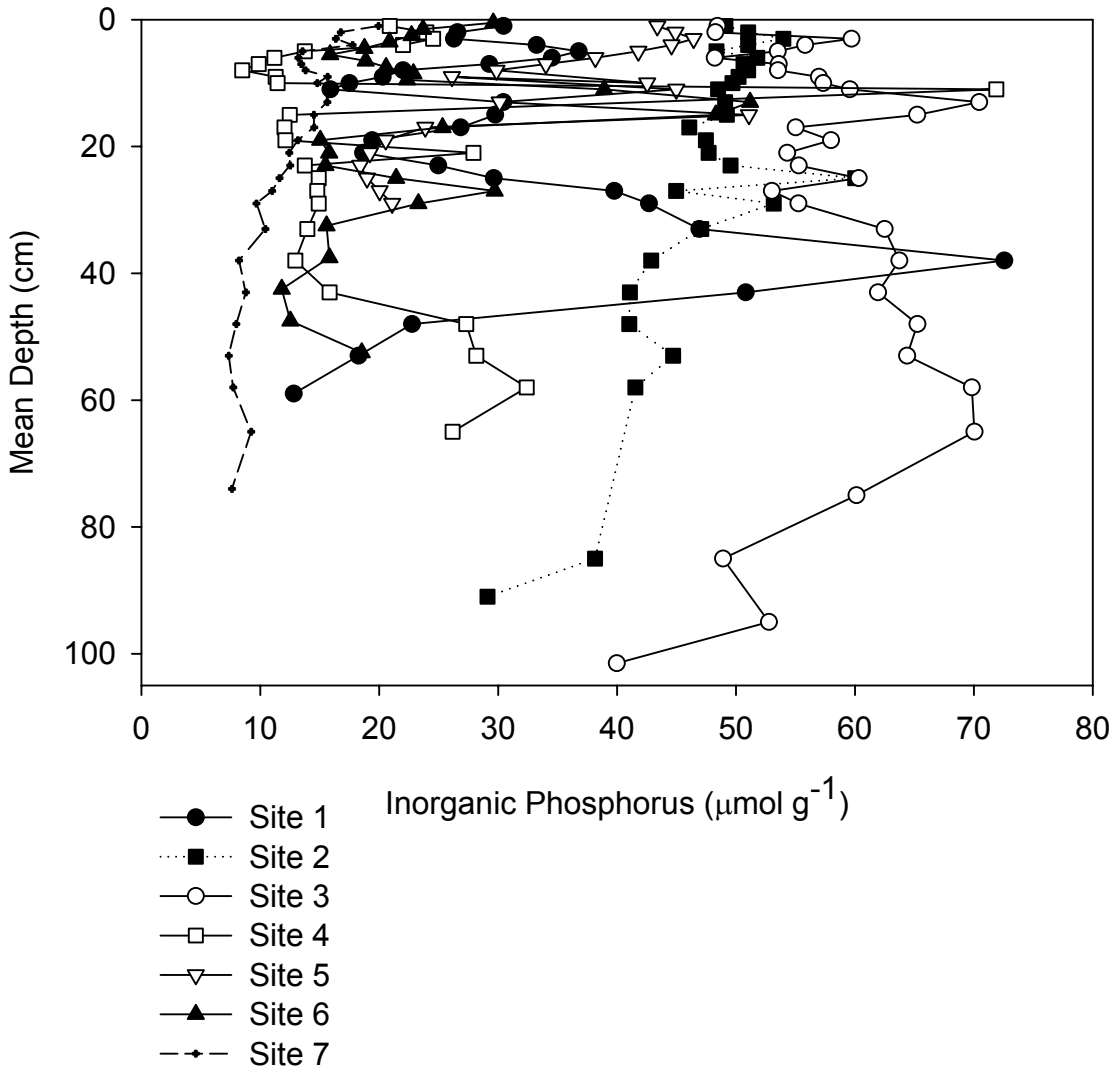

REFERENCES

Adeslon, J. 1997. The evaluation of geochemical indicators of anoxia in The Chesapeake Bay. Ph.D. Dissertation. University of Maryland, College Park, Maryland.

Appleby, P.G., and F. Oldfield. 1978. The calculation of lead-210 dates assuming a constant rate of supply of unsupported ^{210}Pb to the sediment. *Catena* 5:1-8.

Aspila, K.I., H. Agemian, and A. S. Y. Chau. 1976. A semi-automated method for the determination of inorganic, organic and total phosphate in sediments. *Analyst* 101: 187-197.

Berner, R.A. 1964. An idealized model of dissolved sulfate distribution in recent sediments. *Geochimica et Cosmochimica Acta* 28: 1497-1503.

Berner, R.A. 1970. Sedimentary pyrite formation. *American Journal of Science* 265: 773-785.

Berner, R.A., T. Baldwin, and G.R. Holdren Jr. 1979. Authigenic iron sulfides as paleosalinity indicators. *Journal of Sedimentary Petrology* 49(4): 1345-1350.

Blomqvist, S., A. Gunnars, and R. Elmgren. 2004. Why the limiting nutrient differs between temperate coastal seas and freshwater lakes: A matter of salt. *Limnology and Oceanography* 46(6): 2236-2241.

Boynton, W. R., J. H. Garber, R. Summers, and W. M. Kemp. 1995. Inputs, transformations, and transport of nitrogen and phosphorus in Chesapeake Bay and selected tributaries. *Estuaries* 18(1B): 285-314.

Boynton, W. R., J. D. Hagy, J. C. Cornwell, W. M. Kemp, S. Greene, M. Owens, J. Baker, R. Larsen, A. Voinov, and T. Horton. Nutrient inputs, transport, storages, recycling, internal losses and management action in the Patuxent River Estuary. *In Preparation*.

Bratton, J.F., S.M. Colman, and R.R. Seal. 2003. Eutrophication and carbon sources in Chesapeake Bay over the past 2700yr: human impacts in context. *Geochimica et Cosmochimica Acta* 67(18): 3385-3402.

Breitburg, D. L., A. Adamack, K. A. Rose, S E. Kolesar, M. B. Decker, J. E. Purcell, J. E. Keister, and J. H. Cowan Jr. 2003. The pattern and influence of low dissolved oxygen in the Patuxent River, a seasonally hypoxic estuary. *Estuaries* 26(2A):280-297.

Canavan, R. W., and C. P. Slomp. 2007. Phosphorus cycling in the sediment of a coastal freshwater lake and response to salinization. *In Preparation*.

Canfield, D. E., R. Raiswell, and S. Bottrell. 1992. The reactivity of sedimentary iron minerals toward sulfide. *American Journal of Science* 292: 659-683.

Canfield, D. E., R. Raiswell, J. T. Westrich, C. M. Reaves, and R. A. Berner. 1986. The use of chromium reduction in the analysis of reduced inorganic sulfur in sediments and shales. *Chemical Geology* 54: 149-155.

Capone, D.G. and R. P. Kiene. 1988. Comparison of microbial dynamics in marine and freshwater sediments: Contrasts in anaerobic carbon catabolism. *Limnology and Oceanography* 33(4): 725-749.

Caraco, N., J. Cole, and G. E. Likens. 1990. A comparison of phosphorus immobilization in sediments of freshwater and coastal marine systems. *Biogeochemistry* 9: 277-290.

Colman, S.M., and J.F. Bratton. 2003. Anthropogenically induced changes in sediment biogenic silica fluxes in Chesapeake Bay. *Geology* 31(1):71-74.

Conley, D. J. 1988. Biogenic silica as an estimate of siliceous microfossil abundance in Great Lake sediments. *Biogeochemistry* 6:161-179.

Conley, D. J., C. L. Schelske, and E. F. Stoermer. 1993. Modification of the biogeochemical cycle of silica with eutrophication. *Marine Ecology Progress Series* 101:179-192.

Cloern, J. E. 2001. Our evolving conceptual model of the coastal eutrophication problem. *Marine Ecology Progress Series* 210: 223-253.

Cooper, S. R. 1999. The history of water quality in North Carolina estuarine waters as documented in the stratigraphic record. Annual report prepared for the Water Resources Research Institute of the University of North Carolina. Raleigh, North Carolina.

Cooper, S. R., and G. S. Brush. 1991. Long-term history of Chesapeake Bay anoxia. *Science* 254(5034): 992-996.

Cornwell, J. C. 1987. Phosphorus cycling in arctic lake sediments: adsorption and authigenic minerals. *Archiv fur Hydrobiologia* 109: 161-179.

Cornwell, J. C., D. J. Conley, M. Owens, and J. C. Stevenson. 1996. A sediment chronology of the eutrophication of Chesapeake Bay. *Estuaries* 19(2B):488-499.

Cornwell, J.C. and J.W. Morse. 1987. The characterization of iron sulfide minerals in anoxic marine sediments. *Marine Chemistry* 22: 193-206.

Cornwell, J.C., and P.A. Sampou. 1995. Environmental controls on iron sulfide mineral formation in a coastal plain estuary. IN: Vairavamurthy, M.A., M. A. A. Schoonen, T. I.

Eglinton, G. W. Luther III, and B. Manowithz (eds.), *Geochemical transformations of sedimentary sulfur.* Washington, DC: American Chemical Society, pp.224-242.

D'Elia, C. F., W. R. Boynton, and J. G. Sanders. 2003. A watershed perspective of nutrient enrichment, science, and policy in the Patuxent River, Maryland: 1960-2000. *Estuaries* 26(2A):171-185.

DeMaster, D.J. 1981. The supply and accumulation of silica in the marine environment. *Geochimica et Cosmochimica Acta* 45:1715-1732.

Fisher, T.R., J. D. Hagy III, W. R. Boynton, and M. R. Williams. 2006. Cultural eutrophication in the Choptank and Patuxent estuaries of Chesapeake Bay. *Limnology and Oceanography* 51(1, part 2): 435-447.

Froelich, P. N. 1988. Kinetic control of dissolved phosphate in natural waters: A primer on the phosphate buffer mechanism. *Limnology and Oceanography* 33(4): 649-668.

Gagnon, C., A. Mucci, and É Pelletier. 1995. Anomalous accumulation of acid-volatile sulphides (AVS) in coastal marine sediment, Saguenay Fjord, Canada. *Geochimica et Cosmochimica Acta* 59(13): 2663-2675.

Gerritse, RG. (1999). Sulphur, organic carbon and iron relationships in estuarine and freshwater sediments: Effects of sedimentation rate. *Applied Geochemistry* 14: 41-52.

Greene, S. E. 2005. Nutrient removal by tidal fresh and oligohaline marshes in a Chesapeake Bay tributary. M.S. Thesis. University of Maryland, College Park, Maryland.

Hagy, J. D., L. P. Sanford, and W. R. Boynton. 2000. Estimation of net physical transport and hydraulic residence times for a coastal plain estuary using box models. *Estuaries* 23: 328-340.

Howarth, R.W. 1984. The ecological significance of sulfur in the energy dynamics of salt marsh and coastal marine sediments. *Biogeochemistry* 1: 5-27.

Howarth, R. W., and R. Marino. 2006. Nitrogen as the limiting nutrient for eutrophication in coastal and marine ecosystems: Evolving views over three decades. *Limnology and Oceanography* 51(1): 364-376.

Hyacinthe, C., and P. Van Cappellen. 2004. An authigenic iron phosphate phase in estuarine sediments: composition, formation, and chemical reactivity. *Marine Chemistry* 91: 227-251.

Jordan, T.E., D. E. Weller, and D. L. Correll. 2003. Sources of nutrient inputs to the Patuxent River estuary. *Estuaries* 26(2A): 226-243.

Jordan, T.E., J.C. Cornwell, W. R. Boynton, and J. T. Anderson. 2007. Changes in phosphorus biogeochemistry along an estuarine salinity gradient: The iron conveyor belt. *Limnology and Oceanography* In Press.

Kemp, M. W., and W. R. Boynton. 1984. Spatial and temporal coupling of nutrient inputs to estuarine primary production: The role of particulate transport and decomposition. *Bulletin of Marine Science* 35(3): 522-535.

Kemp, M.W., W. R. Boynton, J. E. Adolf, D. F. Boesch, W. C. Boicourt, G. Brush, J. C. Cornwell, T. R. Fisher, P. M. Glibert, J. D. Hagy, L. W. Harding, E. D. Houde, D. G. Kimmel, W. D. Miller, R. I. E. Newell, M. R. Roman, E. M. Smith, E.M., and J. C. Stevenson. 2005. Eutrophication of Chesapeake Bay: Historical trends and ecological implications. *Marine Ecological Progress Series* 303: 1-29.

Khan, H. and G.S. Brush. 1994. Nutrient and metal accumulation in a freshwater tidal marsh. *Estuaries* 17(2):345-360.

Kim, G., N. Hussain, J.R. Scudlark, and T.M. Church. 2000. Factors influencing the atmospheric depositional fluxes of stable Pb, ^{210}Pb, and ^{7}Be into Chesapeake Bay. *Journal of Atmospheric Chemistry* 36:65-79.

Krom, M. D. and R. A. Berner. 1980. Adsorption of phosphate in anoxic marine sediments. *Limnology and Oceanography* 25(5): 797-806.

Lane, L. S., Rhoades, C. Thomas, and L. Van Heukelem. 2000. Standard operating procedures. Horn Point Laboratory. Technical Report No. TS-264-00.

Leventhal, J. and C. Taylor. 1990. Comparison of methods to determine degree of pyritization. *Geochimica et Cosmochimica Acta* 54: 2621-2625.

Lord, C. J. III, and T. M. Church. 1983. The geochemistry of salt marshes: Sedimentary iron diffusion, sulfate reduction, and pyritization. *Geochimica et Cosmochimica Acta* 47: 1381-1391.

Lung, W. S., and S. Bai. 2003. A water quality model for the Patuxent Estuary: Current conditions and predictions under changing land-use scenarios. *Estuaries* 26 (2A): 267-279.

Maryland Department of Planning. 2000. Land Use/Land Cover. (http://www.mdp.state.md.us/info/newmaps/pax2_y2k.htm)

Merrill, J. Z. 1999. Tidal freshwater marshes as nutrient sinks: Particulate nutrient burial and denitrification. Ph.D. Dissertation. University of Maryland, College Park, Maryland.

Merrill, J.Z., and J.C. Cornwell. 2000. The role of oligohaline and tidal freshwater marshes in estuarine nutrient cycling. In: Weinstein, M., and Kreeger, D.A. (eds.),

Concepts and Controversies in Tidal Marsh Ecology. Dordrecht: Kluwer Press, pp.425-441.

Morse, J.W., and J. C. Cornwell. 1987. Analysis and distribution of iron sulfide minerals in recent anoxic marine sediments. *Marine Chemistry* 22: 55-69.

Najjar, R. G. 1999. The water balance of the Susquehanna River Basin and its response to climate change. *Journal of Hydrology* 219: 7-19.

Nixon, S. Q. 1995. Coastal marine eutrophication: A definition, social causes, and future consequences. *Ophelia* 41: 199-219.

Parsons, T.R., Y. Maita, and C.M. Lalli. 1984. *A manual of chemical and biological methods for seawater analysis*. New York: Pergamon Press, 173pp.

Rabouille, C., F.T. Mackenzie, and L.M.Ver. 2001. Influence of the human perturbation on carbon, nitrogen, and oxygen biogeochemical cycles in the global coastal ocean. *Geochimica et Cosmochimica Acta* 65(21):3615-3641.

Raiswell, R., F. Buckley, R. A. Berner, and T. F. Anderson. 1988. Degree of pyritization of iron as a paleoenvironmental indicator of bottom-water oxygenation. *Journal of Sediment Petrology* 58(5): 812-819.

Rickard, D., and J. W. Morse. 2005. Acid volatile sulfide (AVS). *Marine Chemistry* 97 (3-4): 141-197.

Robbins, J. A., D. N. Edgington, and A. L. W. Kemp. 1978. Comparative ^{210}Pb, ^{137}Cs and pollen geochronologies of sediments from Lakes Ontario and Erie. *Quaternary Research* 10:256-278.

Roden, E.E., and J. H. Tuttle. 1993. Inorganic sulfur turnover in oligohaline estuarine sediments. *Biogeochemistry* 22: 81-105.

Rozan, T.E., M. Taillefert, R. E. Trouwborst, B. T. Glazer, S. Ma, J. Herszage, L. M. Valdes, K. S. Price, and G. W. Luther III. 2002. Iron-sulfur-phosphorus cycling in the sediments of a shallow coastal bay: Implications for sediment nutrient release and benthic macroalgal blooms. *Limnology and Oceanography* 47(5): 1346-1354.

Smith, V.H. 2006. Response of estuarine and coastal marine phytoplankton to nitrogen and phosphorus enrichment. *Limnology and Oceanography* 21(1 part 2):377-384.

Sprague, L. A., M. J. Langland, S. E. Yochum, R. E. Edwards, J. D. Blomquist, S. W. Philips, G. W. Shenk, and S. D. Preston. 2000. Factors affecting nutrient trends in major rivers of the Chesapeake Bay watershed. Water-Resources Investigations Report 00-4218. U.S. Geological Survey, Denver, Colorado.

Stankelis, R.M., M.D Naylor, and W.R. Boynton. 2003. Submerged aquatic vegetation in the mesohaline region of the Patuxent Estuary: Past, present, and future status. *Estuaries* 26(2A):186-195.

Testa, J.M. 2006. Factors regulating variability in water quality and net biogeochemical fluxes in the Patuxent River Estuary. M.S. Thesis. University of Maryland, College Park, Maryland.

Weller, D. E., T. E. Jordan, D. L. Correll, and Z. Liu. 2003. Effects of land-use change on nutrient discharges from the Patuxent River watershed. *Estuaries* 26(2A): 244-266.

Weston, N. B., R. E. Dixon, and S. B. Joye. 2006. Ramifications of increased salinity in tidal freshwater sediments: Geochemistry and microbial pathways of organic matter mineralization. Journal of Geophysical Research 111: 1-14.

Westrich, J.T., and R. A. Berner. 1984. The role of sedimentary organic matter in bacterial sulfate reduction: The *G* model tested. *Limnology and Oceanography* 29(2): 236-249.

Zimmerman, A.R., and E. A. Canuel. 2000. A geochemical record of eutrophication and anoxia in Chesapeake Bay sediments: Anthropogenic influence on organic matter composition. *Marine Chemistry* 69: 117-137.

Zimmerman, A.R., and E. A. Canuel. 2002. Sediment geochemical records of eutrophication in mesohaline Chesapeake Bay. *Limnology and Oceanography* 47(4): 1084-1093.